Chapter 5
Design for Body Torsion

In this chapter we consider the overall body structure being twisted. As we did with the bending in Chapter 4, we will consider two types of body torsion requirements: strength and stiffness.

5.1 Body Torsion Strength Requirement

In defining the torsion strength requirement, we are seeking a vehicle-use condition which applies a maximum torque to the body, and yet a condition where the user would expect the body to recover its shape with little to no permanent deformation upon removal of the torque. The *twist ditch* maneuver is such a condition. Here, one wheel falls into a ditch and becomes unsupported, Figure 5.1. Putting the vehicle into static equilibrium for this condition, we see the twist ditch torque, T_{MAX}, is given by

$$T_{MAX} = W_{AXLE} \frac{t}{2} \tag{5.1}$$

where:

W_{AXLE} = Weight for the axle with the highest static load,

t = Track for that axle.

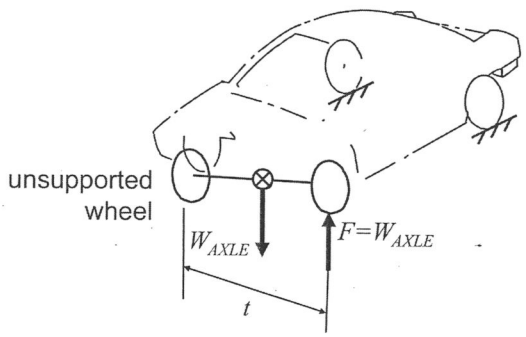

Figure 5.1 Body loaded in twist ditch condition.

A test set-up for this strength requirement is shown in Figure 5.2. The vehicle is supported at the suspension attachment points at one end, and loaded at the suspension attachment points at the other end. At the loaded end an upward deflection, δ, is imposed on one side and an equal downward deflection imposed on the other side, producing a twisting couple. Load cells at the loaded end measure the magnitude of the twisting couple. The angle of twist of the body, ϕ, is also measured as

$$\phi = \frac{2\delta}{w} \tag{5.2}$$

where:

δ = Deflection at each loaded suspension attachment

w =Width at the loaded points

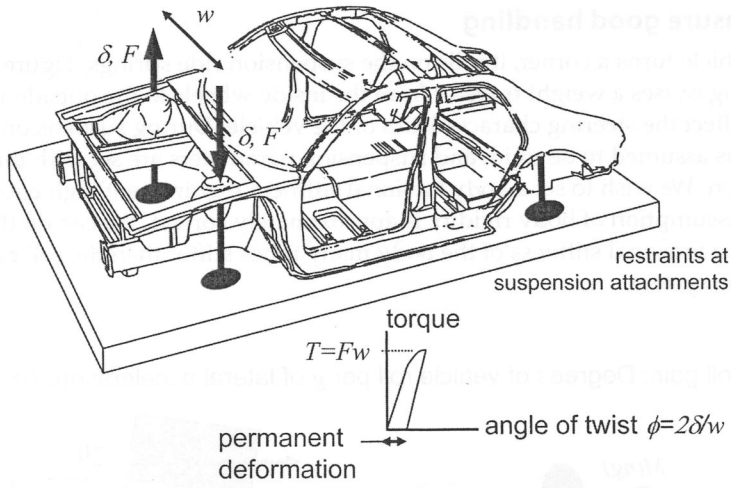

Figure 5.2 Torsion test convention.

For this requirement, we expect the body to suffer little permanent deformation after the twist ditch torque is removed. The chart in Figure 5.3 shows the twist ditch torques for a range of vehicles.

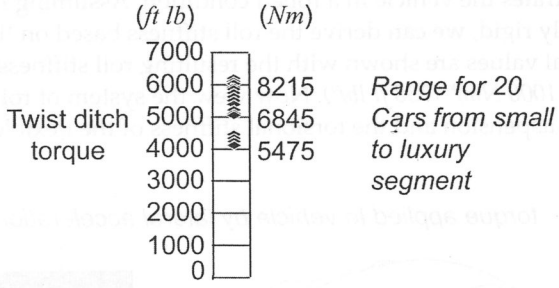

Figure 5.3 Torsion strength benchmarking.

5.2 Body Torsion Stiffness Requirement

From the body torsion test, we can measure a torsion stiffness—the slope in the linear region of the applied couple vs. angular rotation, ϕ. We will now develop the rationale for a body torsion stiffness requirement. Two important functions require high torsional stiffness:

1. To ensure good handling properties, the body should be torsionally stiff relative to the suspension stiffness [1].
2. To ensure a solid structural feel and minimize relative deformations which result in squeaks and rattles.

5.2.1 Ensure good handling

As the vehicle turns a corner, it rolls on the suspension ride springs, Figure 5.4. This rolling causes a weight transfer from the inside wheels to the outside wheels and can affect the steering characteristics of the vehicle. During suspension design, the body is assumed to be rigid, and suspension parameters are set with this assumption. We wish to set a body torsional stiffness requirement high enough such that this assumption of body rigidity is approximately correct. We can do this by making the torsional stiffness of the body many times stiffer than the roll rate of the suspension system.

Roll gain: Degrees of vehicle roll per g of lateral acceleration: θ/n

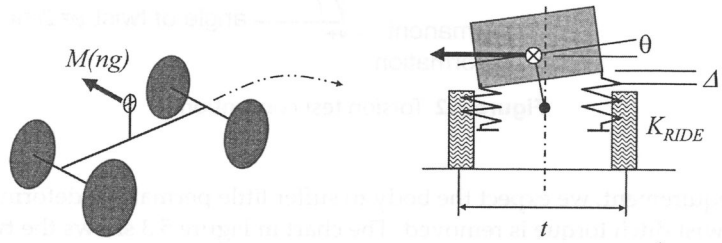

Figure 5.4 Vehicle roll stiffness.

Figure 5.5 illustrates the vehicle in a rolled condition. Assuming for now that the body is infinitely rigid, we can derive the roll stiffness based on the ride spring rates [2]. Typical values are shown with the resulting roll stiffness, K_{ROLL}, equal to approximately *1000 Nm/° (738 ft lb/°)*. Now view the system of roll springs of the front and rear suspension and the torsional stiffness of the flexible body as a series

torque applied to vehicle by lateral acceleration

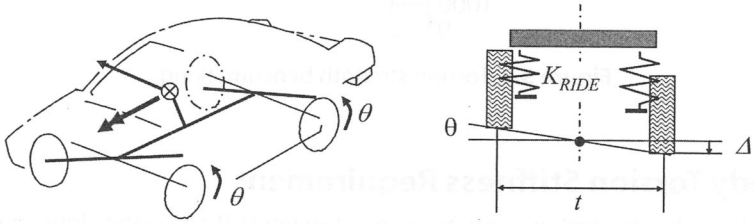

$$K_{ROLL} = K_{ROLL\ FRONT} + K_{ROLL\ REAR} = \frac{t^2 K_{RIDE\ FRONT}}{2} + \frac{t^2 K_{RIDE\ REAR}}{2}$$

typical values:

$t = 1560\ mm$

$K_{RIDE} = 23.4\ N/mm$

$K_{ROLL} = 57000\ Nm/rad = 1000\ Nm/deg$

Figure 5.5 First-order estimate of vehicle roll stiffness.

connection of springs, Figure 5.6. We wish to have the stiffness of this spring system, which includes the torsionally flexible body, Figure 5.6b, approximately equal to the ideal system consisting of only the suspension roll rates, Figure 5.6a. The graph of Figure 5.7 plots the ratio of the stiffness with a torsionally flexible body, K_{EFF}, to the suspension stiffness with a rigid body, K_{ROLL}, against the ratio of body torsional stiffness to suspension roll stiffness. We wish to have K_{EFF}/K_{ROLL} to approach one. Therefore we need the body torsional stiffness, K_{BODY}, to be *10* times the suspension roll stiffness, K_{ROLL}, to achieve $K_{EFF}/K_{ROLL}=0.9$. For typical passenger cars, this places a torsional stiffness requirement at $K_{BODY}=10000\ Nm/^{o}$ *(7375 ft lb/°)* for suspension handling reasons.

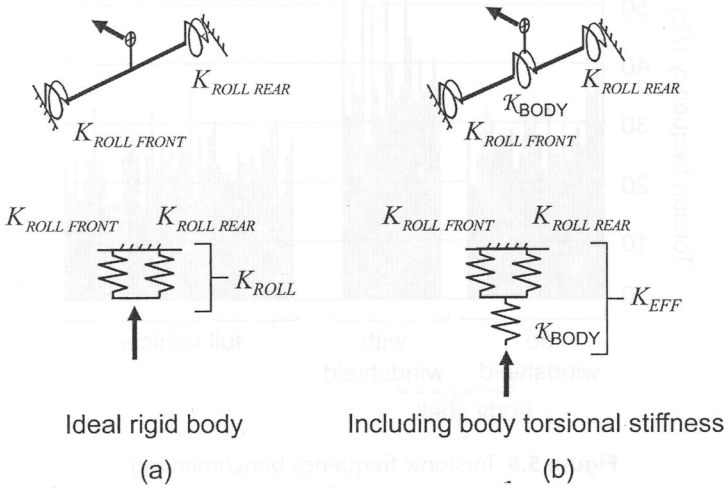

Figure 5.6 Vehicle roll stiffness with torsionally flexible body.

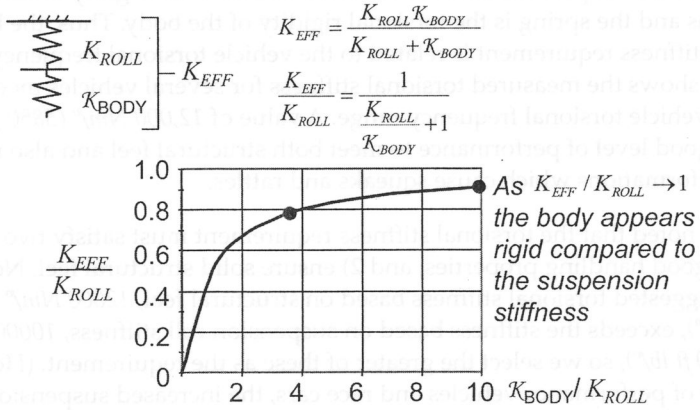

Figure 5.7 Effective torsional rate of flexible body and suspension.

5.2.2 Ensure solid structural feel

The second vehicle function demanding high torsional stiffness is to ensure the feel of solidness over road irregularities. This is related to the fundamental natural frequency of the body twisting mode; in general, higher natural frequency yields a more desirable solid feel. Figure 5.8 shows benchmark torsional resonant frequency data for several vehicles. As with bending vibration, sufficiently solid feel results when the vehicle torsional frequency is in the *22 to 25 Hz* range.

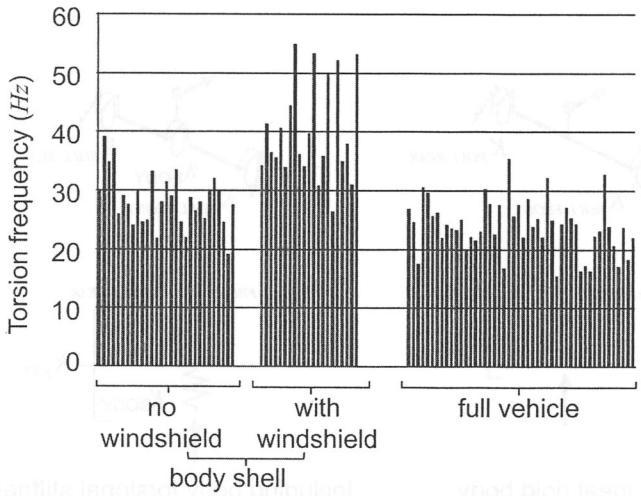

Figure 5.8 Torsional frequency benchmarking.

Consider the torsional resonance as a single-degree-of-freedom mass-spring oscillator where the point mass is the effective inertia of the rigidly attached vehicle subsystems and the spring is the torsional rigidity of the body. Thus, the body torsional stiffness requirement is related to the vehicle torsional frequency target. Figure 5.9 shows the measured torsional stiffness for several vehicles meeting this desirable vehicle torsional frequency range. A value of *12,000 Nm/° (8850 ft lb/°)* is seen as a good level of performance to meet both structural feel and also minimize relative deformations which cause squeaks and rattles.

Earlier we noted that the torsional stiffness requirement must satisfy two functions: 1) ensure good handling properties, and 2) ensure solid structural feel. Note that the suggested torsional stiffness based on structural feel, *12000 Nm/° (8850 ft lb/°)*, exceeds the stiffness based on suspension roll stiffness, *10000 Nm/° (7400 ft lb/°)*, so we select the greater of these as the requirement. (However, in the case of performance vehicles and race cars, the increased suspension roll stiffness of these vehicles makes the suspension stiffness function the dominant requirement for torsion.)

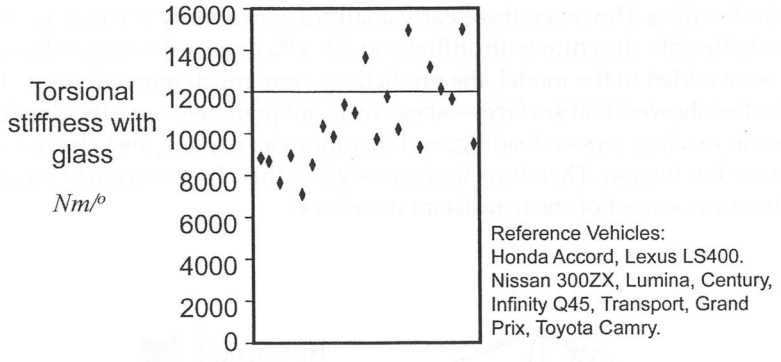

Figure 5.9 Torsional stiffness test and benchmarking. (Courtesy of the American Iron and Steel Institute, UltraLight Steel Auto Body)

To summarize, we have shown how both strength and stiffness requirements may be established for body torsion. Typical values for these requirements are shown in Figure 5.10 for a midsize vehicle. We will now look at the design of body structure to meet these requirements. The next section treats design for the strength requirement, followed by a section on design for the stiffness requirement.

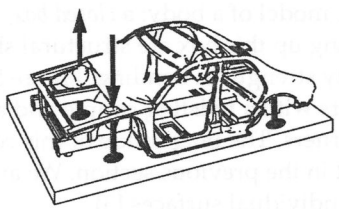

Torsion Strength
nominal value
$T = 6250\ Nm$
no permanent deformation

Torsion Stiffness
nominal value
$\mathcal{K} = 12000\ Nm/°$

Figure 5.10 Typical torsional requirement for a mid-size vehicle.

5.3 Internal Loads During Global Torsion: Load Path Analysis

First we will consider the design of structure to meet the body strength requirement. As with the bending case, our objective is to understand how this global body requirement flows down to loads on structure elements. Once we have the loads on individual structural elements, we can then design those elements using the principles of Chapter 3.

5.3.1 Shear-resistant members

Early computer modeling of body torsional behavior during the 1970s idealized the structure as a framework of beams, Figure 5.11, very similar to our side-frame

model for bending. However, these early analyses consistently predicted a more torsionally flexible structure with stiffness at *10–30%* of experimental values. When panels were added to the model, the predictions were much more accurate. These early studies showed that surfaces—shear-resistant members—are the dominant structure in reacting torsion loading, and that they can explain the behavior of the body loaded in torsion. Therefore, in the models of this chapter we will idealize the body structure as a set of shear-resistant members.

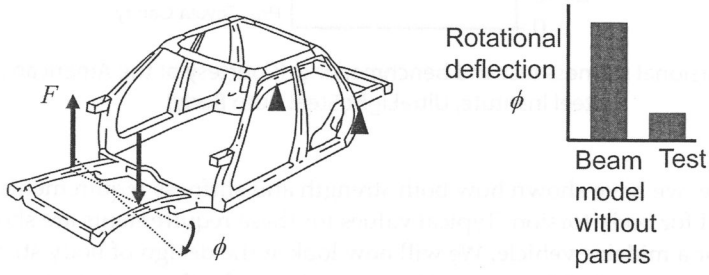

Figure 5.11 Beam model without panels.

We will begin by looking at a very simple model of a body: a *closed box*, Figure 5.12. The structural elements making up this box are structural shear surfaces first introduced in our analysis of the body strength in bending, Figure 5.13. We imagine the box loaded at the front corners with a twisting couple and an equal and opposite couple acting on the rear corners. The magnitude of this couple is the torsional strength requirement developed in the previous section. We are interested in how these applied loads flow into the individual surfaces [3].

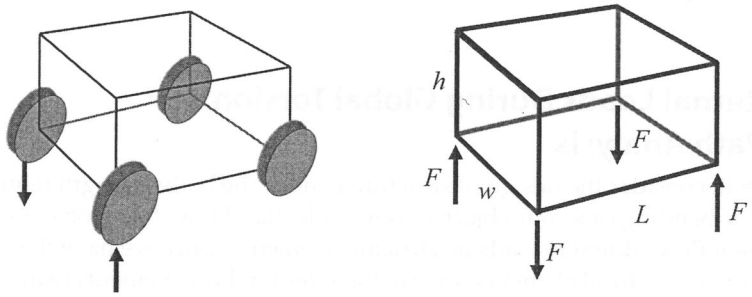

Figure 5.12 Box model.

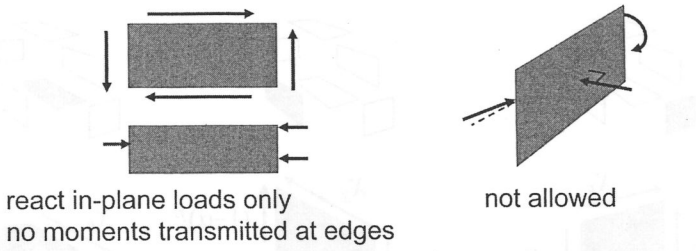

Figure 5.13 Idealized surface element.

Now let us explode the box and look at the internal loads on each surface, Figure 5.14. These loads can be determined, as we did with the bending strength analysis, by setting each surface into static equilibrium [4]. To begin, look the front left applied force. It must be reacted by both the front surface left edge and the side surface front edge, as shown in Figure 5.14b. Let α be the fraction of the applied load taken by the front surface, and $(\alpha-1)$ the fraction taken by the side surface where $0<\alpha<1$. Now set the front surface and side surfaces into equilibrium by taking moments at a corner, Figure 5.15a and b. Finally, consider the bottom surface equilibrium. The forces on this surface must be equal and opposite to those applied by the front surface (along the front edge), and by the side surface (along the side edge), Figure 5.15c. Equilibrium of the bottom then tells us that $\alpha=1/2$ or the applied force is shared equally by the front and side surfaces, regardless of the dimensions of the box.

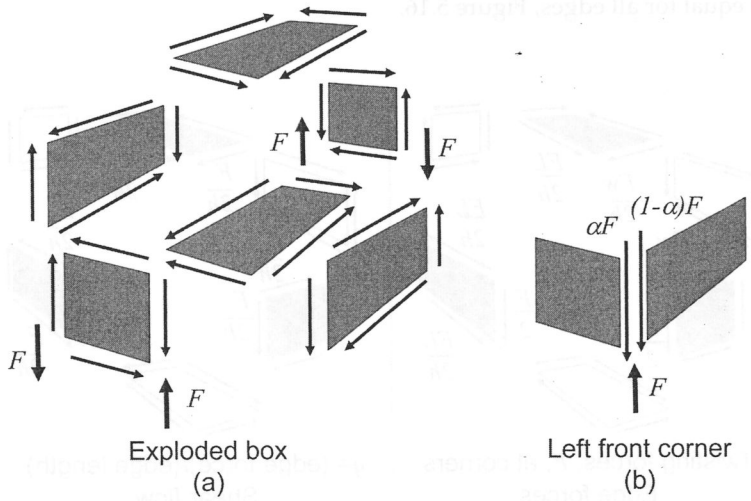

Figure 5.14 Box model internal loads.

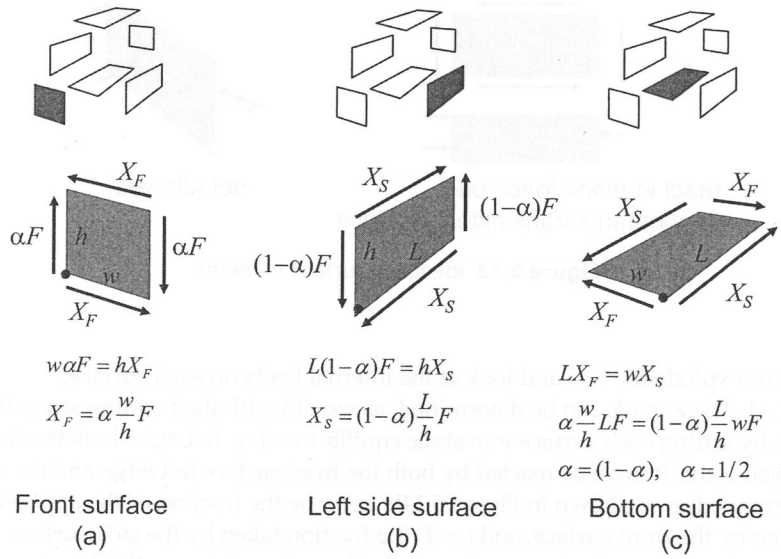

Figure 5.15 Free body of box model.

From the analysis of this simple structure under torsional loading, we see that 1) *all* surfaces are loaded, 2) that the internal loads are independent of material properties, and 3) that each surface is necessary to react the applied torsional couple: removal of any single surface will not allow the required equilibrium and the box will collapse. Also note that the *shear flow*—the shear force per unit of length of the edge it acts upon—is equal for all edges, Figure 5.16.

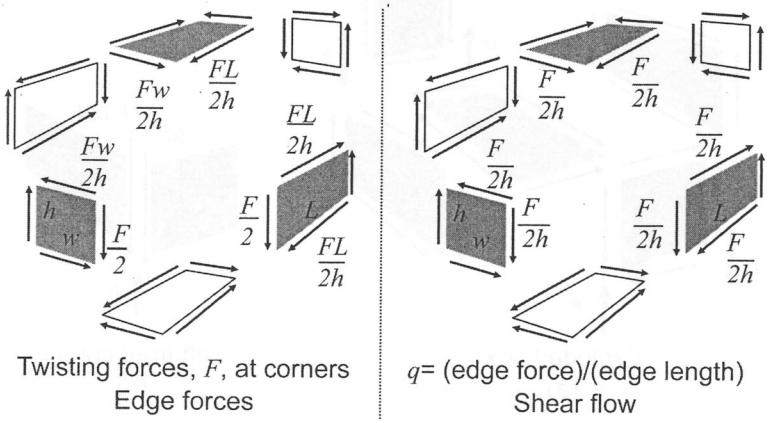

Figure 5.16 Monocoque box in torsion.

Example: Shear loads on rear hatch opening

Even with such a simple model, we can determine internal shear loads within a body structure. Consider the van shown in Figure 5.17 and loaded by the twist ditch torque. We are interested in the shearing loads which need to be reacted by the rear hatch structure, Figure 5.17a. First we must convert the torque requirement to a force couple using $F=T/w$. Using the equations developed for our box model, we immediately find that the shearing loads on the back structural shear surface are as shown in Figure 5.17b. With this information, we could begin to develop a rear hatch structure which will react these shear loads without excessive permanent deformation.

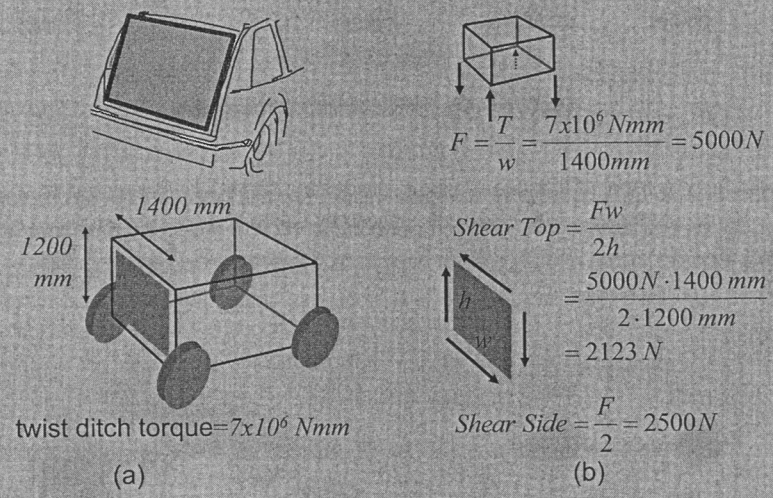

Figure 5.17 Example: Van rear hatch opening.

Note that the shear-resistant structural elements representing each face of the box do not have to be flat surfaces, as we have shown in the illustration of Figure 5.13. A shear-resistant member is any element which can resist the match-boxing deformation shown in Figure 5.18 top. This could be a flat panel as we have shown, a crowned panel, a panel with a hole or ribs, or a framework of beams, Figure 5.18 bottom. Examples of shear-resistant beam frameworks include the side-frame, rear hatch opening, and windshield ring, among others. Less-conventional shear-resistant members include diagonal straps in which only the strap under tension reacts the shear loads, and panels which have been loaded beyond their shear buckling load. Such buckled panels will still resist shearing deformation, with the buckled waves acting as tension members—this state is referred to as *diagonal tension*.

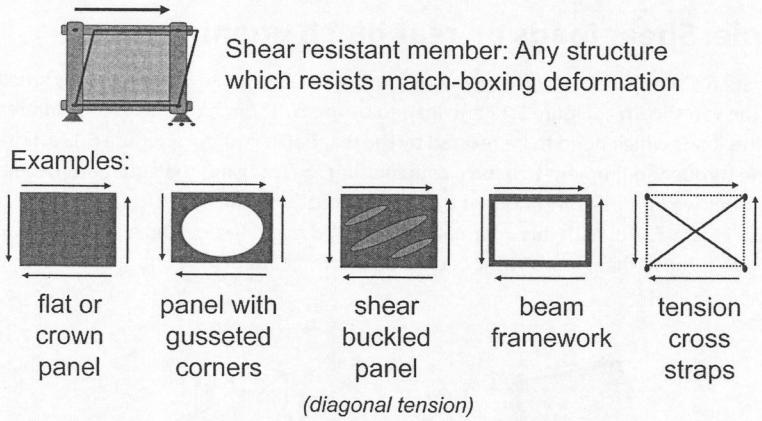

Figure 5.18 Shear-resistant members.

In preparation to look at a more realistic model for the body subjected to torsion loading, let us consider a box-shaped passenger cabin loaded by a torque at the front face and an equal and opposite torque at the rear face, Figure 5.19a.

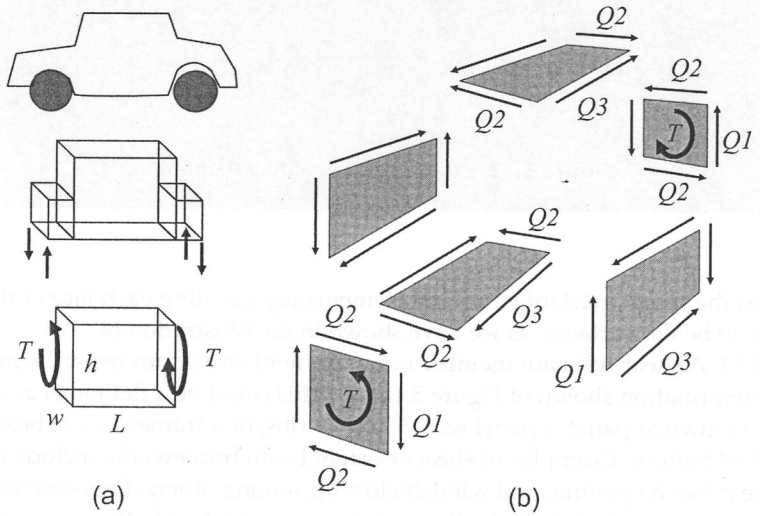

Figure 5.19 Passenger cabin internal loads.

We again place each surface into static equilibrium, Figure 5.19b, but this time we will use a matrix formulation [5]. The three independent equilibrium equations can be written as

$$+wQ_1 + hQ_2 = T \qquad \text{equilibrium of front face}$$

$$-LQ_2 + wQ_3 = 0 \qquad \text{equilibrium of top face}$$

$$-LQ_1 + hQ_3 = 0 \qquad \text{equilibrium of side face}$$

We can now define a column matrix of applied torques

$$\mathbf{T} = \begin{bmatrix} T \\ 0 \\ 0 \end{bmatrix}, \tag{5.3}$$

a column matrix of shear loads

$$\mathbf{Q} = \begin{bmatrix} Q_1 \\ Q_2 \\ Q_3 \end{bmatrix}, \tag{5.4}$$

and a coefficient matrix

$$\mathbf{A} = \begin{bmatrix} \mathbf{w} & \mathbf{h} & \mathbf{0} \\ \mathbf{0} & \mathbf{-L} & \mathbf{w} \\ \mathbf{-L} & \mathbf{0} & \mathbf{h} \end{bmatrix}. \tag{5.5}$$

With these definitions, the equilibrium equations can be written as

$$\mathbf{AQ=T} \tag{5.6}$$

and as we are interested in the internal shear loads, this can be solved as

$$\mathbf{Q=A^{-1}T} \tag{5.7}$$

which gives for this case:

$$\begin{bmatrix} Q_1 \\ Q_2 \\ Q_3 \end{bmatrix} = \frac{1}{2whL} \begin{bmatrix} hL & h^2 & -hw \\ wL & -wh & w^2 \\ L^2 & Lh & Lw \end{bmatrix} \begin{bmatrix} T \\ 0 \\ 0 \end{bmatrix}$$

$$\text{or } Q_1 = \frac{T}{2w}, \quad Q_2 = \frac{T}{2h}, \quad Q_3 = \frac{TL}{2wh}$$

We now have the tools to allow us to look at the more realistic model for the body subjected to torsion loading, Figure 5.20. This is the same shear surface and bar model we used in the analysis of bending loads. Now we will apply the twist ditch torque as force couple, $R_F = T_{MAX}/w'$, acting on the motor compartment side surfaces. An equal and opposite couple is applied to the rear surfaces to place the body system into equilibrium. The model is now exploded, and the unknown internal loads drawn with the assumed positive directions, Figure 5.21. Note that

the loads are symmetrically opposite about the plane dividing the body into right and left sides. As in the bending case, we begin by examining a surface which has an external load applied: the right motor compartment side surface ***a***.

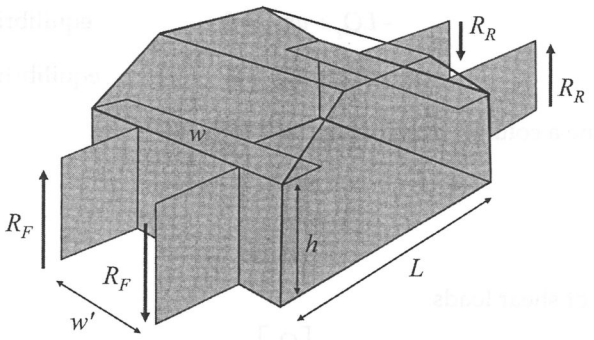

Figure 5.20 Structural surface and bar model.

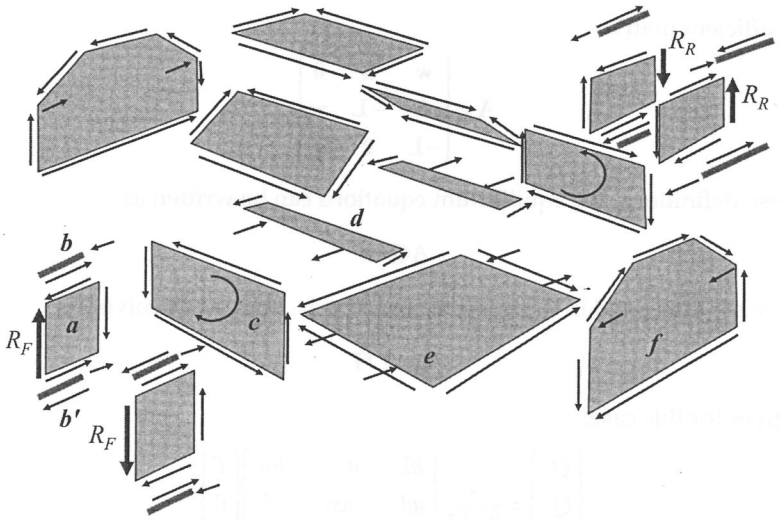

Figure 5.21 Internal loads under twist ditch load.

Proceeding by placing surface ***a*** into equilibrium, we find the internal shearing load, Q, on the top and bottom edges, Figure 5.22. The load on the upper edge is reacted by the bar, ***b***, and we see a load, P_B, is required at its end to place the bar into equilibrium. Similarly, the load on the bottom edge of the surface is reacted by bar, ***b´***.

As in the bending case, we see the motor compartment side, surface ***a***, is loaded in shear, and we can use the principles developed in Chapter 3 to design this panel to meet these shear loads. As the magnitude of shear loads differs from the bending case, the worst case—bending or torsion—is used to size the panel.

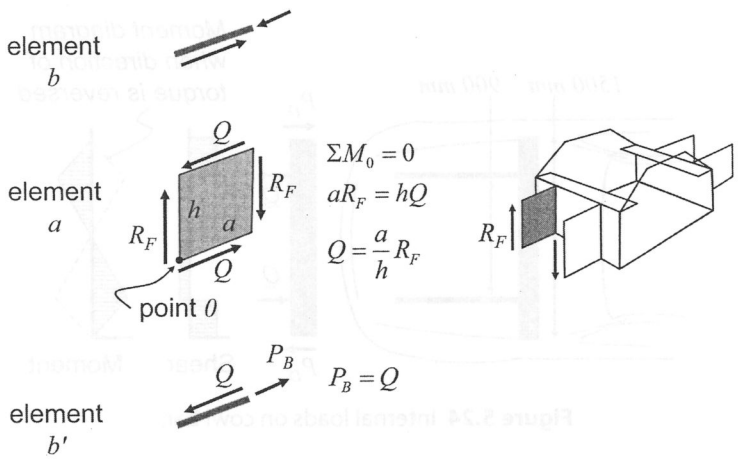

Figure 5.22 Internal loads on motor compartment panel.

Isolating the cowl surface, surface ***d*** in Figure 5.23, we see a rearward load applied by the left bar ***b*** and, due to asymmetry, an equal forward load applied by the right bar. To place the cowl surface into equilibrium, equal and opposite loads, P_D, are applied at the ends of the cowl. We can now identify all the loads applied to the cowl during twist ditch torsion loading, and can determine the moment diagram shown in Figure 5.24. We can now design a cowl section to react these moments without failing. With a thin-wall section, we must account for buckling, and determine if the elements of the section in compression are buckled. But we must note that the twist ditch torsion load may be in either the clockwise or counterclockwise direction. Therefore the moments on the cowl may be reversed in sign, and the compressed side of the section reversed. The designed section must accommodate both conditions.

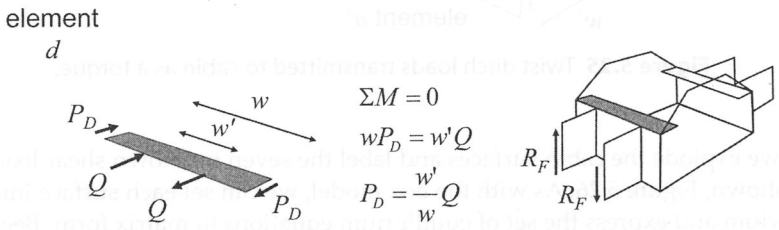

Figure 5.23 Internal loads on cowl and package shelf.

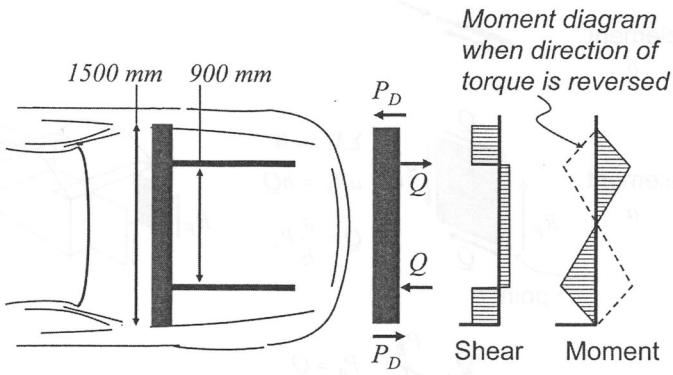

Figure 5.24 Internal loads on cowl bar.

We can now turn our attention to the cabin surfaces, Figure 5.25. Note that, like our earlier simple model of a six-sided box, the cabin forms a space totally enclosed by surfaces, although now we have eight sides. The cabin is loaded by a twisting couple applied to the dash by the motor compartment sides, ***a*** and ***a´***. The couple has the same magnitude as the twist ditch torque. A similar, but opposite, arrangement occurs at the rear of the cabin structure with the couple applied to the rear surface.

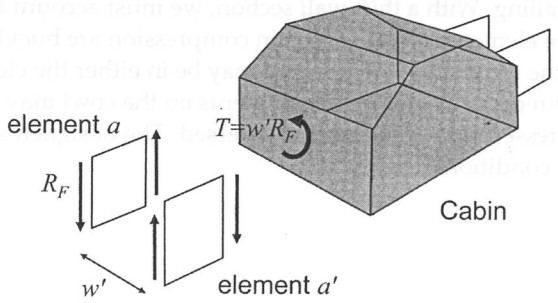

Figure 5.25 Twist ditch loads transmitted to cabin as a torque.

Again we explode the cabin surfaces and label the seven unknown shear loads, Q_1 to Q_7, as shown, Figure 5.26. As with the box model, we can set each surface into static equilibrium and express the set of equilibrium equations in matrix form. Beginning with the dash surface with an external torque applied, we sum moments about a corner point and set to zero,

$$h_1Q_1+wQ_2-T=0 \qquad \text{equilibrium of dash surface}$$

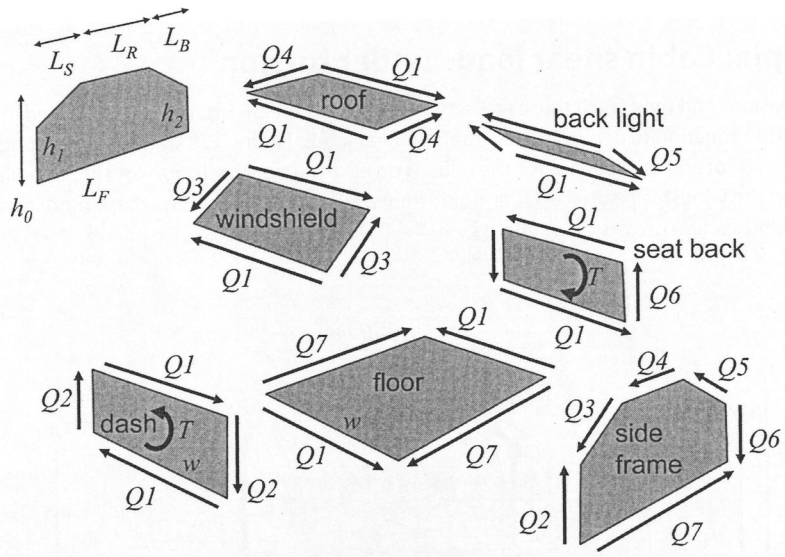

Figure 5.26 Shear loads on cabin panels.

Proceeding with equilibrium equations for all seven surfaces (only one side surfaces gives an independent equation), we end up with seven linear equations with seven unknown shear loads. These equations may be expressed in matrix form as we did with the simple six-sided box case in Equations 5.3 though 5.6:

$$\begin{bmatrix} h_1 & w & 0 & 0 & 0 & 0 & 0 \\ L_S & 0 & -w & 0 & 0 & 0 & 0 \\ L_R & 0 & 0 & -w & 0 & 0 & 0 \\ L_B & 0 & 0 & 0 & -w & 0 & 0 \\ h_2 & 0 & 0 & 0 & 0 & w & 0 \\ L_F & 0 & 0 & 0 & 0 & 0 & -w \\ 0 & 0 & 0 & (h_o - h_1) & \left[L_F(h_o - h_2) + L_2(h_2 - h_1)\right] / L_B & -L_F & h_1 \end{bmatrix} \begin{bmatrix} Q_1 \\ Q_2 \\ Q_3 \\ Q_4 \\ Q_5 \\ Q_6 \\ Q_7 \end{bmatrix} = \begin{bmatrix} T \\ 0 \\ 0 \\ 0 \\ T \\ 0 \\ 0 \end{bmatrix} \begin{matrix} \text{dash} \\ \text{windshield} \\ \text{roof} \\ \text{backlight} \\ \text{rear seat panel} \\ \text{floor} \\ \text{side frame} \end{matrix} \quad (5.8)$$

In this set of equations, **AQ=T**, the applied torque is known and we wish to find the internal shearing loads Q_1 to Q_7. With the cabin dimensions, we can substitute numerical values for the coefficient matrix, **A**, and solve for the shearing loads, $\mathbf{Q=A^{-1}T}$.

Several important points should be made on determining internal shear loads:

1. The loads were identified independently of material, so whether steel, aluminum, plastic or other, the structural elements must react these loads under body torsion
2. Each surface must be present to react its loads, otherwise the body will collapse
3. Each structural surface has the ability to react shear loads, and the actual structural element can be a beam framework, a curved panel, or others as discussed previously and shown in Figure 5.18.

Example: Cabin shear loads under torsion

The dimensions and twist ditch torque for a typical mid-size sedan, Figure 5.27, were used in the above matrix equation to determine the internal shear loads. Figure 5.28 shows the resulting matrix formulation (top) and the solution for shear loads on each surface (bottom). Note in particular the loading on the windshield surface, Q_1, and side frame, Q_7, as we will examine these more closely in the following section on torsional stiffness.

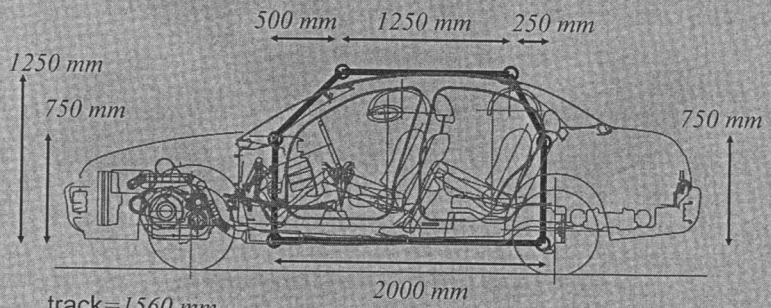

Figure 5.27 Example sedan data. (Courtesy of the American Iron and Steel Institute, UltraLight Steel Auto Body)

$$
\underset{\mathbf{A}}{\begin{bmatrix} 750 & 1560 & 0 & 0 & 0 & 0 & 0 \\ 707 & 0 & -1560 & 0 & 0 & 0 & 0 \\ 1250 & 0 & 0 & -1560 & 0 & 0 & 0 \\ 559 & 0 & 0 & 0 & -1560 & 0 & 0 \\ 750 & 0 & 0 & 0 & 0 & 1560 & 0 \\ 2000 & 0 & 0 & 0 & 0 & 0 & -1560 \\ 0 & 0 & 0 & 500 & 1789 & -2000 & 750 \end{bmatrix}}
\underset{\mathbf{Q}}{\begin{bmatrix} Q1 \\ Q2 \\ Q3 \\ Q4 \\ Q5 \\ Q6 \\ Q7 \end{bmatrix}} =
\underset{\mathbf{T}}{\begin{bmatrix} 7730000 \\ 0 \\ 0 \\ 0 \\ 7730000 \\ 0 \\ 0 \end{bmatrix}}
$$

$$
\underset{\times 10^{-4}\,\mathbf{A}^{-1}}{\begin{bmatrix} 0 & 0 & 1.081 & 3.868 & 4.324 & 1.622 & 3.373 \\ 6.410 & 0 & -0.520 & -1.860 & -2.079 & -0.780 & -1.622 \\ 0 & -6.410 & 0.490 & 1.753 & 1.960 & 0.735 & 1.529 \\ 0 & 0 & -5.544 & 3.099 & 3.465 & 1.299 & 2.703 \\ 0 & 0 & 0.387 & -5.024 & 1.550 & 0.581 & 1.209 \\ 0 & 0 & -0.520 & -1.860 & 4.331 & -0.780 & -1.622 \\ 0 & 0 & 1.386 & 4.959 & 5.544 & -4.331 & 4.324 \end{bmatrix}}
\underset{\mathbf{T}}{\begin{bmatrix} 7.73x10^6 \\ 0 \\ 0 \\ 7.73x10^6 \\ 0 \\ 0 \\ 0 \end{bmatrix}} =
\underset{\mathbf{Q}}{\begin{bmatrix} 3343 \\ 3348 \\ 1515 \\ 2678 \\ 1198 \\ 3348 \\ 4286 \end{bmatrix}}
\begin{matrix} Q_1 \\ Q_2 \\ Q_3 \\ Q_4 \\ Q_5 \\ Q_6 \\ Q_7 \end{matrix}
$$

Figure 5.28 Shear loads for example sedan.

5.3.2 Summary: Torsion strength

In this section, we have shown how the applied torque in the global torsion strength test can be *flowed down* to the shear loads on each individual structural element. To accomplish this flow down of requirements, we used a model consisting of simple structural surfaces and bar elements, Figure 5.26. We set each element into static equilibrium to find a set of equations for the shear loads, set them into matrix form, and solved by inverting the coefficient matrix, Equation 5.8. Then, knowing the subsystem loads, the section design principles developed in the Chapter 3 can be used to find the appropriate structural elements to react these loads. We have thus gone from a torsion strength requirement on the body system to ensuring the strength of each structural element under torsion.

5.4 Analysis of Body Torsional Stiffness

In the previous section we examined how the torsion strength requirement implies loading on each structural element, and how we can ensure that each element is sufficiently strong. We will now focus on the global torsion stiffness requirement and flow down the requirement to shear stiffness requirements of the individual structural elements.

We begin by looking again at the six-sided box model, but now we look at the elastic angular deflection of the box under a torsional load, T, Figure 5.29. The angular deflection, θ, is the relative rotation between the front and rear surfaces. The torsional stiffness of the box, K, is the ratio T/θ. We wish to develop an equation which will predict torsional stiffness given the box dimensions, surface thicknesses, and material properties. To do this we will use energy methods, and we first develop an equation for the shear strain energy of a surface [6].

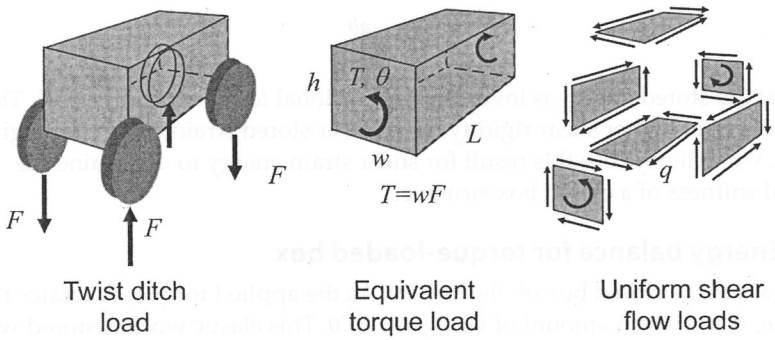

Figure 5.29 Van box model for torsional deformation.

5.4.1 Shear strain energy of a surface

When a surface is loaded in shear, the surface distorts into the diamond shape shown in Figure 5.30, and energy is stored as in an elastic spring. The shear strain energy, *e*, for a surface in uniform shear is given by:

$$e = \int_{VOLUME} \frac{\tau\gamma}{2} dV \tag{5.9}$$

where:

τ = Shear stress

γ = Shear strain

and the integral is over the panel volume.

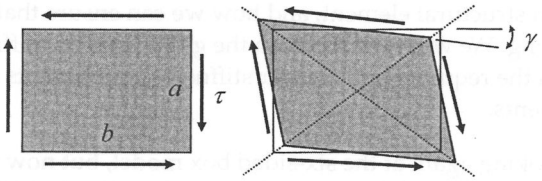

Figure 5.30 Panel under uniform shear.

We assume that the panel is in uniform shear, and both τ and γ are constant over the panel. This equation can be expressed in a useful form in terms of the panel dimensions, *a*, *b*, *t*, the material shear modulus, *G*, and the shear flow, *q*:

$$\tau = \frac{q}{t}, \quad V = abt, \quad \text{and} \quad G = \frac{\tau}{\gamma}, \quad \text{then} \quad e = \int_{VOLUME} \frac{\tau^2}{2G} dV = \frac{\tau^2}{2G} abt$$

$$e = q^2 \frac{ab}{2(Gt)} \tag{5.10}$$

Note that the stored energy is inversely proportional to shear rigidity, *(Gt)*. That is, surfaces with higher shear rigidity have lower stored strain energy for a given loading. We will now use this result for shear strain energy to determine the torsional stiffness of a closed box structure.

5.4.2 Energy balance for torque-loaded box

Look again at the closed box of Figure 5.29. As the applied torque, *T*, rotates through the angle, θ, it does an amount of work, $W=\frac{1}{2}T\theta$. This elastic work is stored within the panels as shear strain energy. By equating external work to the total stored energy, we can determine an expression for rotational deflection:

Work done by external torque = Total shear strain energy in all surfaces

From Equation 5.19,

$$\frac{1}{2}T\theta = \sum_{\text{ALL SURFACES}} \frac{1}{2}q^2\left[\frac{ab}{(Gt)}\right]_{\text{SURFACE i}}$$

Recall that shear flow for a closed box, Figure 5.16, is

$$q = \frac{F}{2h} = \frac{\left(\frac{T}{w}\right)}{2h} = \frac{T}{2wh}$$

Substituting into the above,

$$\frac{1}{2}T\theta = \frac{1}{2}\left(\frac{T}{2wh}\right)^2 \sum_{\text{ALL SURFACES}} \left[\frac{ab}{(Gt)}\right]_{\text{SURFACE i}}$$

$$\theta = T\left(\frac{1}{2wh}\right)^2 \sum_{\text{ALL SURFACES}} \left[\frac{ab}{(Gt)}\right]_{\text{SURFACE i}}$$

$$K = \frac{T}{\theta} = (2wh)^2 \frac{1}{\sum_{\text{ALL SURFACES}} \left[\frac{ab}{(Gt)}\right]_{\text{SURFACE i}}}$$

The important result below gives the torsional stiffness of a closed six-sided box in terms of the properties for each surface.

$$K = (2wh)^2 \frac{1}{\left[\frac{ab}{(Gt)}\right]_{\text{SURFACE 1}} + \left[\frac{ab}{(Gt)}\right]_{\text{SURFACE2}} + \left[\frac{ab}{(Gt)}\right]_{\text{SURFACE 3}} + \left[\frac{ab}{(Gt)}\right]_{\text{SURFACE 4}} + \left[\frac{ab}{(Gt)}\right]_{\text{SURFACE 5}} + \left[\frac{ab}{(Gt)}\right]_{\text{SURFACE 6}}} \tag{5.11}$$

where:

K = Torsional stiffness of box

G = Shear modulus

w = Width of box

h = Height of box

a, b = Dimension of a side surface

t = Thickness of side surface

5.4.3 Series spring analogy

To gain a physical understanding of the way the rigidity, (Gt), for each of the six surfaces combine to give the torsional stiffness of the box, consider a set of six linear springs in series, Figure 5.31. Now look at the mathematical formulation for such springs in series which relates the combined stiffness to the stiffness of each spring:

$$\frac{1}{K_{EQ}} = \frac{1}{K_1} + \frac{1}{K_2} + \frac{1}{K_3} + \frac{1}{K_4} + \frac{1}{K_5} + \frac{1}{K_6}$$

$$K_{EQ} = \frac{1}{\left[\frac{1}{K_1}\right] + \left[\frac{1}{K_2}\right] + \left[\frac{1}{K_3}\right] + \left[\frac{1}{K_4}\right] + \left[\frac{1}{K_5}\right] + \left[\frac{1}{K_6}\right]} \tag{5.12}$$

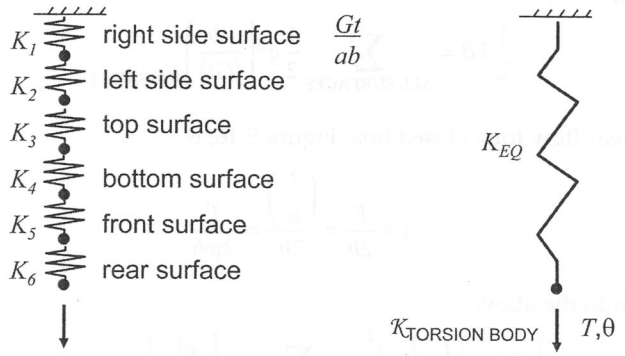

Figure 5.31 Spring analogy for torsional stiffness.

Rearranging the box torsional stiffness equation, Equation 5.11 can be rewritten as:

$$K = (2wh)^2 \frac{1}{\left[\frac{1}{\left(\frac{(Gt)}{ab}\right)}\right]_{SURF\ 1} + \left[\frac{1}{\left(\frac{(Gt)}{ab}\right)}\right]_{SURF\ 2} + \left[\frac{1}{\left(\frac{(Gt)}{ab}\right)}\right]_{SURF\ 3} + \left[\frac{1}{\left(\frac{(Gt)}{ab}\right)}\right]_{SURF\ 4} + \left[\frac{1}{\left(\frac{(Gt)}{ab}\right)}\right]_{SURF\ 5} + \left[\frac{1}{\left(\frac{(Gt)}{ab}\right)}\right]_{SURF\ 6}} \quad (5.13)$$

Compare the form of Equation 5.12 for linear springs in series with Equation 5.13 for our box in torsion. View the quantity $\left(\frac{(Gt)}{ab}\right)$ for each surface in Equation 5.13 as analogous to the stiffness K_i in Equation 5.12, and the forms are the same except for the constant, $(2wh)^2$. It can be seen that each surface of a box in torsion contributes to the torsional stiffness in the same way that each spring contributes to the equivalent stiffness in a series of springs.

As we pull at the end of a series of springs, Figure 5.31, the deflection is dominated by the most flexible spring in the group. If our objective is to increase stiffness, the most efficient way is by increasing the stiffness of the least stiff spring—stiffening the more-stiff springs will do little. This suggests a strategy to meet torsional stiffness requirements:

> *To increase torsional stiffness, identify which surface is the most flexible—lowest* $\left(\frac{(Gt)}{ab}\right)$ *—and improve it.*

Example: Application of torsional stiffness equation

As an example, let us model a van with the dimensions shown in Figure 5.32 as a six-sided box with ideally flat, non-buckling, steel surfaces, *1 mm* thick. Substituting values into Equation 5.13 we find $K=6.95x10^{10}$ *Nm/rad* $=1{,}200{,}000$ *Nm/°*. Comparing this value with the benchmark torsional stiffness data of Figure 5.9, we can see this answer is about *100* times stiffer than measured data! Clearly there is a problem.

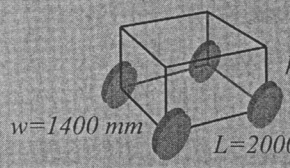

all panels steel
$G=80{,}000\ N/mm^2$
$t=1\ mm$

Surface	$\frac{1}{\left(\frac{Gt}{ab}\right)}(mm/N)$
front and back	$(1250\ mm)(1400\ mm)/(80000\ N/mm)=21.88$
top and bottom	$(2000\ mm)(1400\ mm)/(80000\ N/mm)=35.00$
right and left	$(2000\ mm)(1250\ mm)/(80000\ N/mm)=31.25$

$$K=4(1400\ mm)^2(1250\ mm)^2\ \frac{1}{2(21.88+35+31.25)\ mm^3/N}$$

$$K=6.95x10^{10}\ Nmm/rad\ (1{,}220{,}000\ Nm/^o)$$

Figure 5.32 Example: Torsional stiffness of a box van.

In the above example, the estimated torsional stiffness was *100* times stiffer than anticipated. The problem is not with Equation 5.13 but with our use of ideal flat panels for each surface. In doing so, we have assumed that the surfaces remain perfectly flat during loading. In this unlikely case, the stiffness is very high as anyone who has twisted a closed shoe box knows. In reality, the surfaces of a vehicle body differ considerably from an ideal flat plate; they often have considerable out-of-plane shape such as crown, they have holes and cut-outs, often they are a framework of beams with flexible joints. Despite these realities, Equation 5.13 is still valid if we use the *effective shear rigidity, (Gt)EFF*, for these real surfaces.

5.4.4 Effective shear rigidity for structural elements

Using the *effective shear rigidity*, $(Gt)_{EFF}$, for each real-world panel in Equation 5.13, we can predict torsional stiffness for a body structure. To determine $(Gt)_{EFF}$, we consider the behavior of a test panel in a pinned frame fixture, Figure 5.33. This test fixture is made of four rigid bars connected at their ends by pin joints. Two of the joints are connected to ground, a shearing load is applied at the opposite side, and deflection is measured in line with the load. With no panel in the fixture, it offers no resistance to deformation, and deforms in a diamond shearing shape as shown in Figure 5.33.

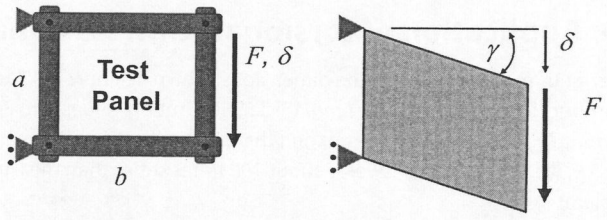

$$(Gt)_{EFF} = \left(\frac{F}{\delta}\right)\left(\frac{b}{a}\right) = S\left(\frac{b}{a}\right)$$ Where S is panel stiffness from test, (F/δ)

Figure 5.33 Test for effective (Gt).

Now consider a flat panel to be connected along the bars, and under load the panel will be deformed in a state of uniform shear, Figure 5.33. We wish to relate the applied load and measured deflection to the shear rigidity, *(Gt)*, of the flat panel. Using the definition of shear modulus, we can arrive at the simple relationship:

$$G = \frac{\tau}{\gamma}, \quad \tau = \frac{F}{at}, \quad \gamma = \frac{\delta}{b}$$
$$(Gt) = \left(\frac{F}{\delta}\right)\left(\frac{b}{a}\right) = S\left(\frac{b}{a}\right), \quad \text{where } S = \left(\frac{F}{\delta}\right) \tag{5.14}$$

Where:

(Gt) = Inferred shear rigidity for the panel

S = Measured stiffness, (slope of the load F vs. deflection δ curve)

a = Panel dimension of the side to which the load is applied

b = Adjacent side dimension

This test suggests a means to determine the effective shear rigidity for any real world-panel: Imagine the panel held in the fixture of Figure 5.33, apply a shearing load, F, and measure the resulting deflection, δ. From the plot of F *vs.* δ, find the stiffness, S (slope). The effective shear rigidity is then given by Equation 5.14. The generation of the stiffness, S, may be determined by an actual physical test, by a strength-of-material type analysis, or by finite element analysis.

Now we have a strategy for calculation of vehicle torsional stiffness: use the surface model of Figure 5.29 and the resulting Equation 5.13 as before, but substitute *effective shear rigidity* for each real-world shear-resistant element as found from Equation 5.14

Examples using effective shear rigidity

To illustrate the use of Equations 5.13 and 5.14 we will look at four shear-resistant members: a van rear hatch perimeter, a general crown panel, the windshield-adhesive system, and the body side frame.

Example: Van rear hatch perimeter

We consider the perimeter of a van rear hatch opening as made of four rigid bars connected by flexible joints, Figure 5.34. If we imagine this model placed in the shear test fixture described above, we can apply basic energy analysis to determine the stiffness. Under a load, F, the frame deflects an amount, δ, and the work done by the external force is

$$w = \frac{1}{2} F\delta$$

This work is stored in each of the corner joints, and equating the external work with the energy stored in the joints, we have

$$\frac{1}{2} F\delta = 4\left(\frac{1}{2} K_J \theta^2\right)$$

Since $\theta = \frac{\delta}{b}$ we have for the stiffness of the framework

$$S = \frac{F}{\delta} = \frac{4k_J}{b^2}$$

Using Equation 5.14, we determine that the effective shear rigidity for the frame is

$$(Gt)_{EFF} = \frac{4k_J}{ab} \tag{5.15}$$

where:

$(Gt)_{EFF}$ = Effective shear rigidity of a rigid frame with flexible joints

k_J = Joint rate

a, b = Dimensions of frame

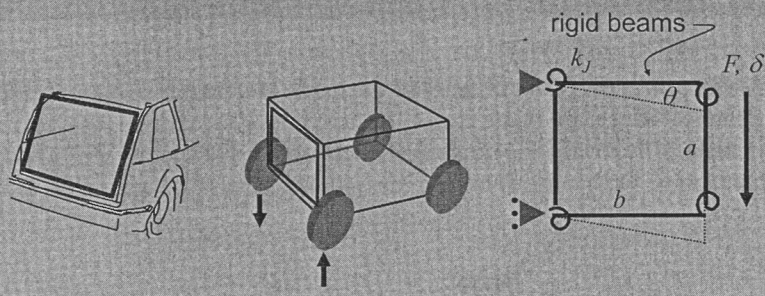

Figure 5.34 Effective shear rigidity of a frame with flexible joints

Let us now apply this result to the torsional stiffness of the box van of Figure 5.32. In that earlier example, each surface was an ideal flat, non-buckling panel. Let us replace the rear panel with an open frame of rigid links with a typical joint stiffness value, $k_J = 0.1 \times 10^8$ *Nmm/rad*

Using Equation 5.15 we find that the effective shear rigidity for the rear opening is

$$(Gt)_{EFF} = \frac{4(0.1 \times 10^8 \, Nmm/rad)}{(1250mm)(1400mm)} = 22.86 N/mm$$

Compare this value to our previous value for the flat, 1-*mm*-thick panel: *(Gt)=(80,000 N/mm)(1 mm)=80,000 N/mm*. So the frame is much more flexible than the original assumption of a flat panel.

Now we can use Equation 5.13 to determine the resulting torsional stiffness for this van made of flat, *1-mm*-thick steel panels *except* for the frame substituted for the rear surface, Figure 5.35. The resulting value for torsional stiffness, Figure 5.35, is much lower than that computed previously for the van with all flat surfaces, Figure 5.32, and more in line with reality. Note that only one surface of the closed box need be flexible to reduce the stiffness for the whole box. This is an illustration of the series spring view of torsional stiffness from Figure 5.31.

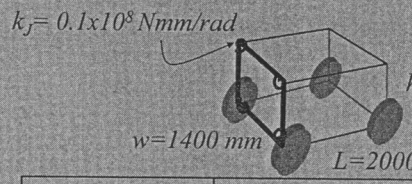

all panels steel
$G=80{,}000\ N/mm^2$
$t=1$ mm

Surface	$\left(\frac{Gt}{ab}\right)^{-1}$ (mm/N)
front	$(1250\ mm)(1400\ mm)/(80000\ N/mm)=21.88$
top and bottom	$(2000\ mm)(1400\ mm)/(80000\ N/mm)=35.00$
right and left	$(2000\ mm)(1250\ mm)/(80000\ N/mm)=31.25$
rear	$(1250\ mm)(1400\ mm)/(\mathbf{22.86\ N/mm})=\mathbf{76553}$

$$K=4(1400\ mm)^2(1250\ mm)^2\left(\frac{1}{(21.88+35+35+31.25+31.25+76553)mm^3/N}\right)$$

$K=1.6x10^8$ Nmm/rad (2807 Nm/°)

Figure 5.35 Example: Van with frame around hatch opening.

The above example shows the influence of the hatch opening on torsional stiffness of a van. In practice, efforts are made to use the hatch door to increase the shear rigidity of the rear surface. Typically, the hinge and latch are not sufficiently stiff to do this, and mechanisms to wedge the door into the opening are used, Figure 5.36 & 5.37.

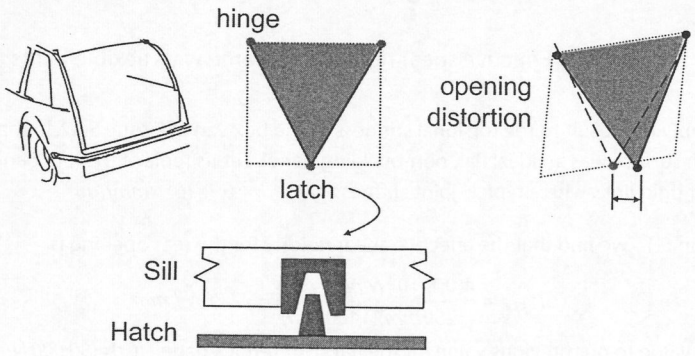

Figure 5.36 Van hatch latch effect on torsional stiffness.

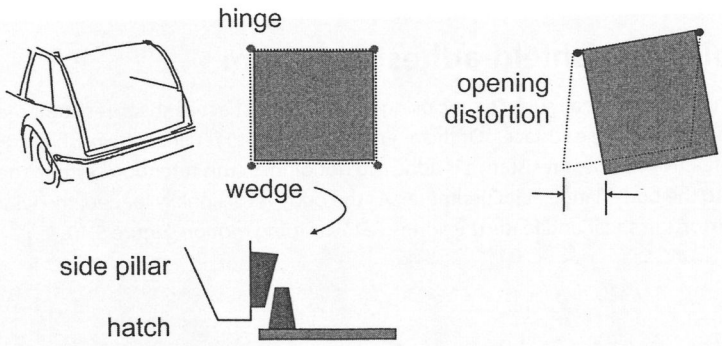

Figure 5.37 Van hatch wedge effect on torsional stiffness.

Example: Crown panel

Many panels on a vehicle are crowned in shape. The reason for this is that the crown shape improves panel stiffness for normal loading such as dent resistance and panel vibration. To determine the effective shear rigidity for panels of various crown heights, an FEA model of the shear test fixture was constructed for typical panel dimensions, Figure 5.38a. The resulting $(Gt)_{EFF}$, Figure 5.38b, shows that for crowns from *10–40 mm*, the $(Gt)_{EFF}$ is much smaller than for a flat panel. This explains why our initial calculation of torsional stiffness using flat panel values gave us unrealistically high values.

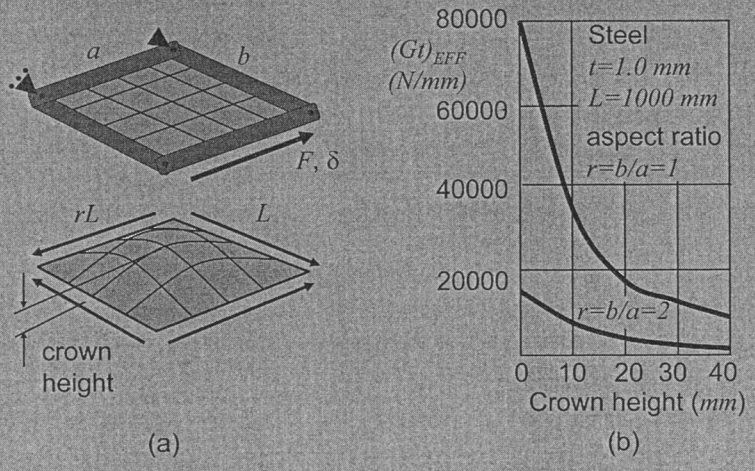

Figure 5.38 Effective shear rigidity of crown panels based on FEA.

Example: Windshield-adhesive system

We now understand that all surfaces enclosing the cabin must act as shear-resistant members. The windshield is one of these surfaces. Of the alternative means to retain the windshield, Figure 5.39, the most effective for shear resistance is adhesive bonding. In this retention system, the windshield is bonded to the body flange at its perimeter. As the body is torsionally loaded, the windshield opening distorts in shear and loads the adhesive in a wiping motion, Figure 5.40.

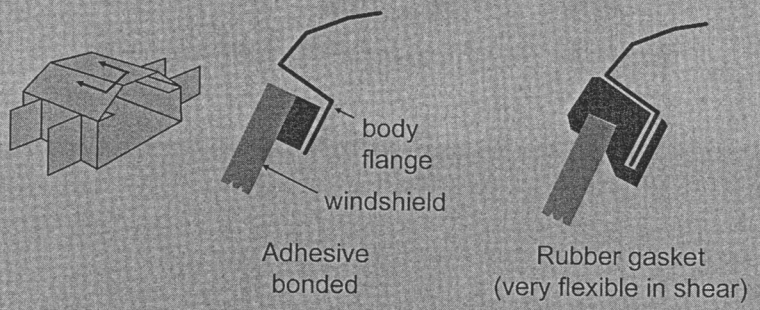

Figure 5.39 Windshield retention alternatives.

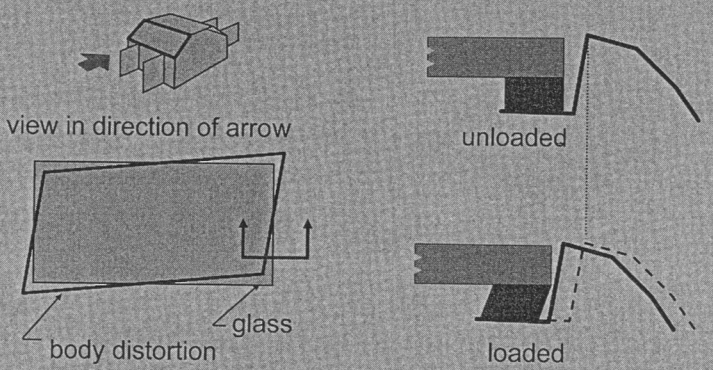

Figure 5.40 Effective shear rigidity of windshield-adhesive system.

A spring system is formed by the three members: the windshield opening frame, the windshield, and the adhesive, as shown in Figure 5.41a. In Figure 5.41b we show the relative shear stiffness for each of these members by itself. As can be seen, the frame is relatively flexible, K_3, and the parallel path of windshield with adhesive, K_7 & K_8, provides the main path for shearing stiffness. As a measure

of this additional stiffness, the torsional resonances are compared with and without windshield glass, Figure 5.42. For many vehicles there is a marked increase in torsional frequency with glass installed, indicating a torsionally stiffer body. For those vehicles which do not show this increase, the body windshield opening perimeter is very stiff.

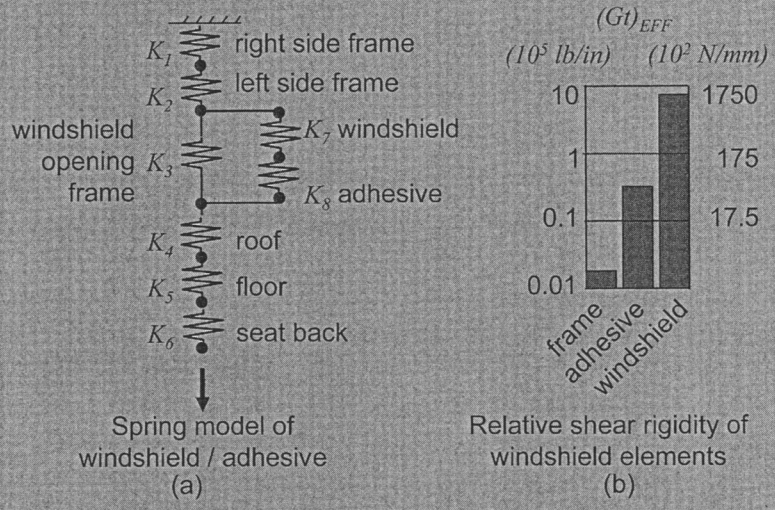

Figure 5.41 Windshield model for torsional stiffness.

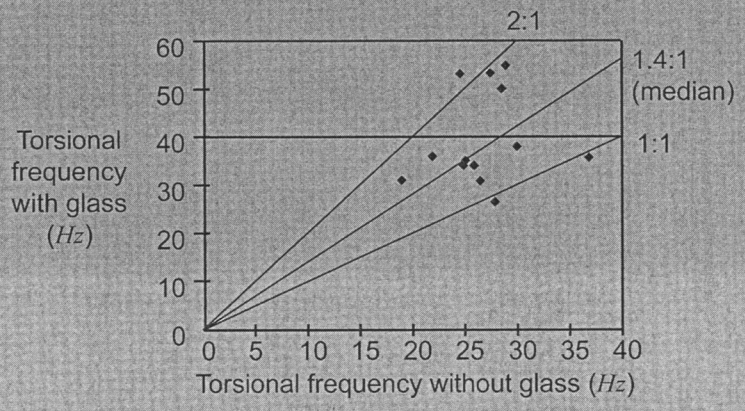

Figure 5.42 Effect of windshield on torsion frequency.

Example: Side frame

In the chapter on bending, we examined the sedan side-frame under bending loads. Now we can look at the influence of side-frame performance on torsional stiffness. We replace the side surfaces in our torsion model with the beam framework of the side-frame, Figure 5.43. We can determine the effective shear rigidity of the side frame by imagining it in the shear test fixture, Figure 5.44. As the side frame is a redundant structure, we use FEA to simulate its behavior in this fixture. We restrain the side-frame at the hinge-pillar-to-rocker joint, and at the rocker-to-C-pillar joint with a pin to ground. We apply a shearing load across the top of the side-frame along the roof rail, Figure 5.45, and solve for the resulting horizontal deflection. Using Equation 5.14 we can then identify the effective shear rigidity for this side-frame as shown at the bottom of Figure 5.45.

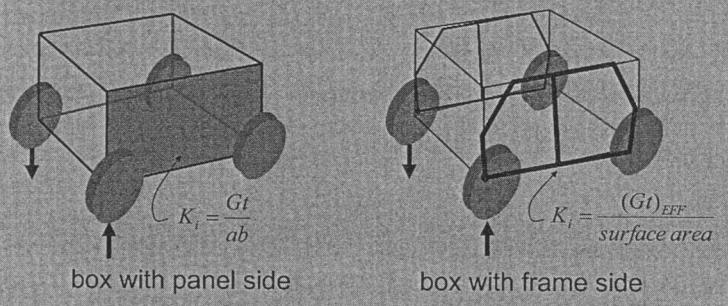

Figure 5.43 Side-frame contribution to torsional stiffness.

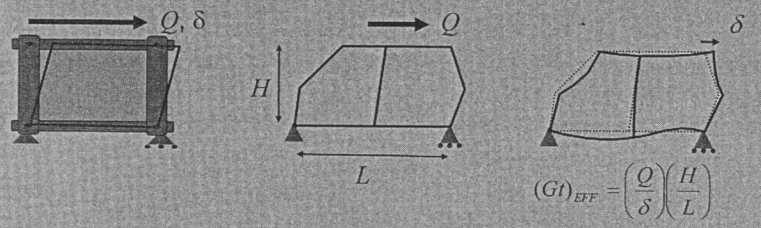

Figure 5.44 Effective shear rigidity of side frame.

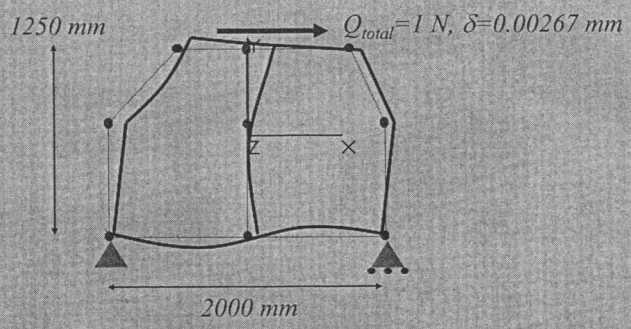

$$(Gt)_{EFF} = \left(\frac{Q}{\delta}\right)\frac{H}{L} = \left(\frac{1N}{.00267mm}\right)\frac{1250mm}{2000mm} = 234N/mm$$

Figure 5.45 Side-frame FEA under shear loading.

Note that this is the same side-frame FEA model used earlier in the bending analysis of Chapter 4. However, the restraints and loading for the torsion case are different, resulting in a different deflected shape and also a different strain energy distribution.

5.4.5 Torsional stiffness of a vehicle cabin

Earlier we looked at the internal loads of a sedan cabin, Figure 5.46. The torsional stiffness of that cabin can be found by generalizing Equation 5.13 from the six-sided box to a cabin with more surfaces enclosing the volume, Figure 5.47. Again, the work done by the external torque will equal the shear strain energy in all surfaces:

$$\frac{1}{2}T\theta = \sum_{\text{ALL SURFACES}} \frac{1}{2}q^2\left[\frac{ab}{(Gt)}\right]_{\text{SURF i}}$$

Dividing both sides by T^2,

$$\frac{\theta}{T} = \left(\frac{q}{T}\right)^2 \sum_{\text{ALL SURFACES}} \left[\frac{\text{area of surface i}}{(Gt)_{EFF}}\right]_{\text{SURF i}}$$

$$K = \frac{1}{\left(\frac{q}{T}\right)^2 \sum_{\text{ALL SURFACES}} \left[\frac{\text{area of surface i}}{(Gt)_{EFF}}\right]_{\text{SURF i}}} \tag{5.16}$$

where (q/T) is found by solving the matrix equation $\mathbf{Q=A^{-1}T}$, Equation 5.7, and q is the resulting shear flow on any non-loaded surface.

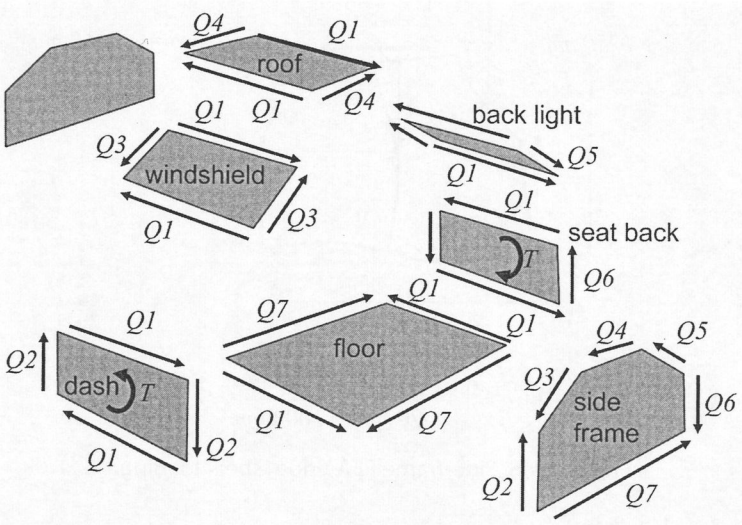

Figure 5.46 Cabin surfaces.

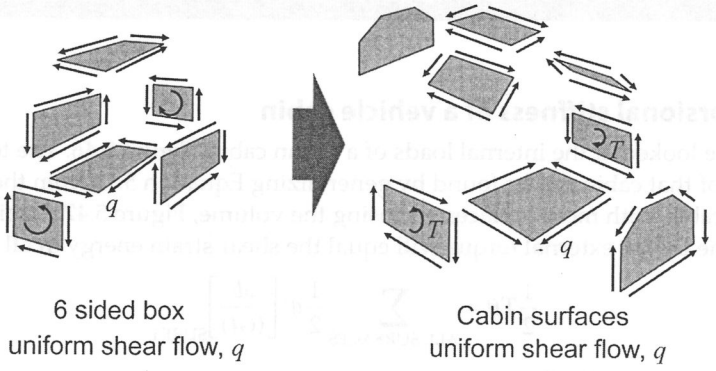

Figure 5.47 Uniform shear flow in cabin.

These relationships provide a calculation procedure for the torsional stiffness of a realistic cabin structure:

1. Apply a torque, T, to the structure and solve for the internal shear loads, Q_i, using $\mathbf{Q=A^{-1}T}$ (An example of this was done in earlier in Figures 5.27 & 5.28 and Equation 5.8.)
2. Find the shear flow, q, by taking any of the surfaces not loaded by the external torque and dividing that shear load by the length of the side over which the load acts. Then form the ratio (q/T) with the torque being the value used in step one
3. Determine the effective shear rigidity, $(Gt)_{EFF}$, for each panel using Equation 5.14
4. Substitute the values for (q/T), $(Gt)_{EFF}$, and surface area into Equation 5.16 to determine the torsional stiffness of the cabin.

Example: Sedan torsional stiffness with side-frame

Let us use the procedure outlined above to determine the cabin torsional stiffness for the sedan cabin dimensions from Figure 5.27. For the two side surfaces, we will use the side-frame described above in "Example: Side frame" and, for simplicity, let all the other surfaces remain flat, *1-mm*-thick steel panels. Proceeding through the four steps outlined above:

1. We can use the results from the torsional strength analysis done earlier for this sedan cabin, Figure 5.28. There we found, for *T=7,730,000 Nmm*, the shear loads, Q_1 through Q_7, which are given in Figure 5.28 with the convention of Figure 5.26. For example, the shear load on the roof panel side is $Q_4=2678\ N$.
2. With the roof panel side length of *1250 mm*, Figure 5.27, we find

$$q=(2678N)/(1250mm)=2.1414N/mm$$

and

$$(q/T)=(2.1414N/mm)/(7{,}730{,}000Nmm)=2.77\times10^{-7}\ mm^{-2}.$$

3. The effective shear rigidity for each side-frame from the previous "Example: Side frame," Figure 5.45, is

$$(Gt)_{EFF}=234\ N/mm$$

and for the other surfaces

$$(Gt)=80{,}000\ N/mm^2(1\ mm)$$

4. Now using Equation 5.16, Figure 5.48, we find that the cabin torsional stiffness is *K=11,423 Nm/°*.

Panel	Area of panel (mm^2)	Effective shear rigidity $(Gt)_{EFF}$ (N/mm)	$\left[\frac{\text{area of surface i}}{(Gt)_{EFF\,i}}\right]$ (mm^3/N)
dash	1170000	80000	14.6
windshield	1103087	80000	13.8
roof	1950000	80000	24.4
back light	872067	80000	10.9
seat back	1170000	80000	14.6
floor	3120000	80000	39.0
side frame-left	2312500	234	9882.5
side frame-right	2312500	234	9882.5
		sum	19882.3

$$K=\frac{1}{\left(\frac{q}{T}\right)^2\sum_{\text{ALL SURFACES}}\left[\frac{\text{area of surface i}}{(Gt)_{EFF\,i}}\right]}=6.55\times10^8\ Nmm/rad\ (11491\ Nm/o)$$

Figure 5.48 Cabin structure torsional stiffness.

If this cabin system stiffness is not adequate with respect to the requirement, we can return to the side-frame FEA of Figure 5.45 and improve the shearing stiffness. Again, we can use strain energy to direct us to the beams and joints which will have the largest impact on improving stiffness.

5.4.6 Summary: Torsion stiffness

We have investigated the torsional behavior of enclosed structures constructed of shear-resistant surfaces. Using energy principles, we developed Equation 5.16, which relates the shear stiffness of the individual surfaces making up the cabin structure to the body torsional stiffness, Figure 5.26. For perfectly flat panels, this shear rigidity is *(Gt)*—the product of shear modulus and thickness. However, for the real surfaces which make up the cabin surfaces, we need to identify the *effective shear rigidity*, $(Gt)_{EFF}$. This is done by visualizing the real surface loaded in a shear test fixture, Figure 5.33. By evaluating the load and deflection in this test fixture, the effective shear rigidity for the panel can be determined using Equation 5.14. As with the strength load case, we found that all surfaces must be present to provide torsional stiffness, and that the least stiff surface dominates the stiffness of the body. A convenient way to visualize the cabin torsional stiffness is as a series combination of springs, with each spring being one panel's effective shear rigidity, Figure 5.31.

5.5 Torsional Stiffness of Convertibles and Framed Vehicles

Our focus in this chapter on torsion has been on the body as a monocoque structure, that is, enclosed by shear-resistant surfaces. This focus is motivated by the efficiency of this type of structure in reacting torsional loading. However, other alternatives exist, Figure 5.49, although they seldom approach the torsional stiffness efficiency achieved by the monocoque structure, Figure 5.50. In this section we will discuss some of the most notable alternative structures.

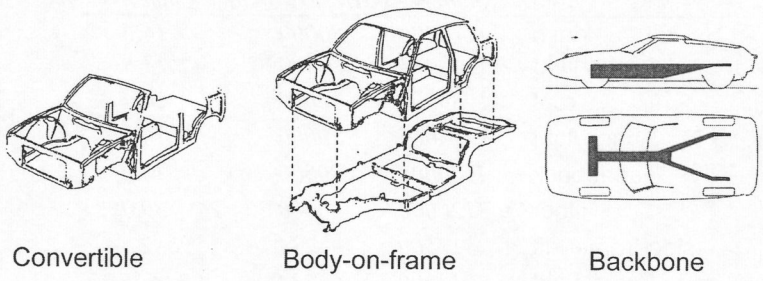

Figure 5.49 Alternatives to monocoque body structure.

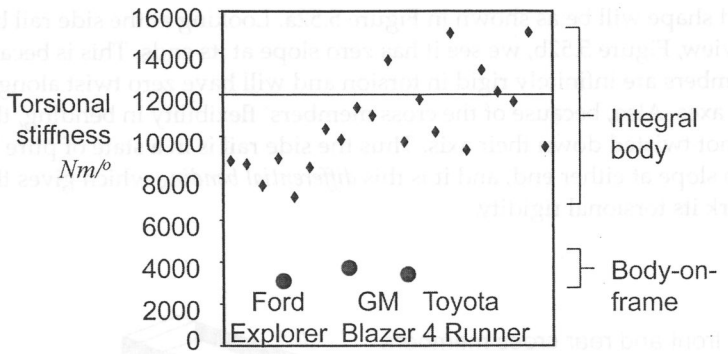

Figure 5.50 Body-on-frame torsional stiffness benchmarking.

5.5.1 Torsional stiffness of convertibles

We have stressed the need for all surfaces of the vehicle body 'box' to be present to react torsional loads. In a convertible, we have removed the top of the box, and lost the ability to react loads via shear resistant surfaces. This can be visualized with the series spring analogy, Figure 5.51, where the series chain is 'broken' with the absence of the top surface. In order to provide adequate torsional rigidity, we add another spring in parallel—a lower load path—to resist torsional loads. A common means to provide this load path is to use *differential bending* of the rocker beams.

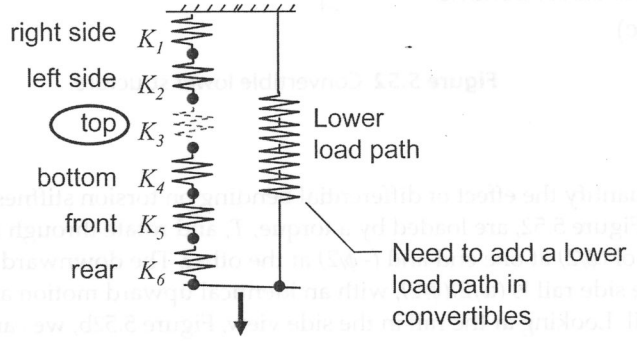

Figure 5.51 Convertibles with top shear-resistant member removed.

Consider the lower structure of a convertible to be idealized as two cross members and two side rail beams, Figure 5.52a. The front cross member shown is located at the dash, and the rear cross member is located at the rear seat back. In this model, both cross members are viewed to be infinitely stiff in torsion about their longitudinal axis, but very flexible in bending. Now let a torque be applied to the front cross member, and a reacting torque applied to the rear cross member. The

deformed shape will be as shown in Figure 5.52a. Looking at the side rail beam in the side view, Figure 5.52b, we see it has zero slope at its ends. This is because the cross members are infinitely rigid in torsion and will have zero twist along their cross-car axes. Also, because of the cross members' flexibility in bending, the side rails are not twisted down their axis. Thus the side rail is in a state of pure bending with zero slope at either end, and it is this *differential bending* which gives this framework its torsional rigidity.

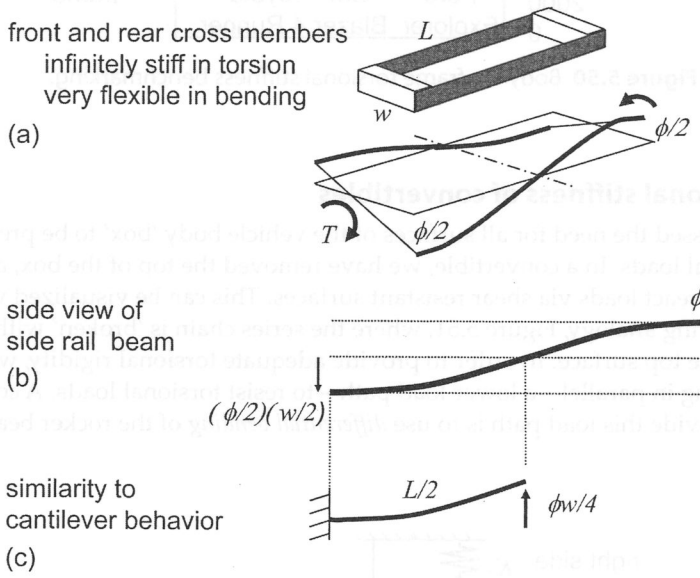

Figure 5.52 Convertible lower structure.

We now quantify the effect of differential bending on torsion stiffness. The structural elements, Figure 5.52, are loaded by a torque, T, and rotate through a total angle, ϕ an angle of $(\phi/2)$ at one end and $(-\phi/2)$ at the other. The downward motion at the front of the side rail is $(w/2)(\phi/2)$, with an identical upward motion at the rear of the side rail. Looking at the rail in the side view, Figure 5.52b, we can see that the behavior for the front half is identical to a cantilever beam of length $(L/2)$, Figure 5.52c. Using the deflection equation for a cantilever

$$Tip\ Defection = \frac{FL^3}{3EI}$$

we can calculate the force, F, required for a deflection of $(w/2)(\phi/2)$.

$$F = 3EI\left(\frac{w\phi}{4}\right)\left(\frac{2}{L}\right)^3$$

This end force appears at both ends of the front cross member, so we have the applied torque needed to achieve the deflection ϕ. This yields a first-order equation for torsional stiffness, K, of a frame with differential bending:

$$\frac{T}{\phi} = \frac{wF}{\phi} = \frac{w}{\phi}\left[3EI\left(\frac{w\phi}{4}\right)\left(\frac{2}{L}\right)^3\right]$$

$$\mathrm{K} = \frac{6w^2EI}{L^3} \tag{5.17}$$

where:

EI = Side rail bending stiffness

L = Length between front and rear cross members

w = Frame width

Example: Torsional stiffness of a frame under differential bending

Considering a frame with a side rail section of *100-mm*-square and *2-mm*-thick steel *(I=1.33x10^6 mm^4)*, with frame width of *1500 mm* and length *3000 mm*, Equation 5.17 yields

$$\mathrm{K} = \frac{6(1500mm)^2(207000N/mm^2)(1.33x10^6 mm^4)}{(3000mm)^3} = 137{,}655{,}000 Nmm/rad$$

or K=*2415 Nm/°* –a low but not unreasonable stiffness.

Differential bending is frequently applied to structure for convertibles. In that application, the torsionally rigid cross members are realized in practice by a large closed box section at the dash and at the rear seat back, Figure 5.53. This approximates the very rigid six-sided box model we have used earlier but on the scale of a cross member rather than the whole cabin. A difficulty with realizing differential bending in practice is the cross-member-to-side-rail joint. The zero-slope end condition in the side rail requires a very large bending moment to be transferred by the cross member, Figure 5.53 bottom. This large moment can cause stress concentrations at the joint, which can lead to durability problems if not treated during design.

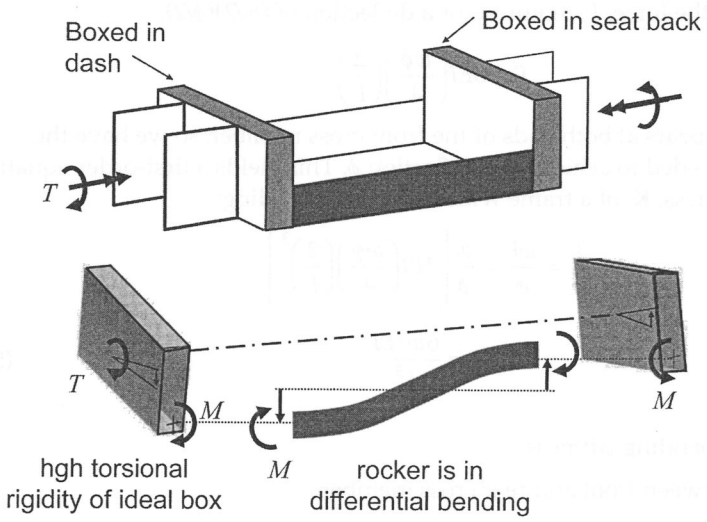

Figure 5.53 Convertible structural elements: Differential bending.

5.5.2 Torsional stiffness of body-on-frame vehicles

A common arrangement for both passenger and utility vehicles is the *body-on-frame* configuration. In this configuration, a body shell is attached to a ladder frame with several elastomeric body mounts, Figure 5.54. These body mounts allow relative motion between the frame and body, both in the vertical direction (compression), and in lateral direction (shear). The primary function of the body mounts is the isolation of structure-borne noise and vibration from the frame into the body.

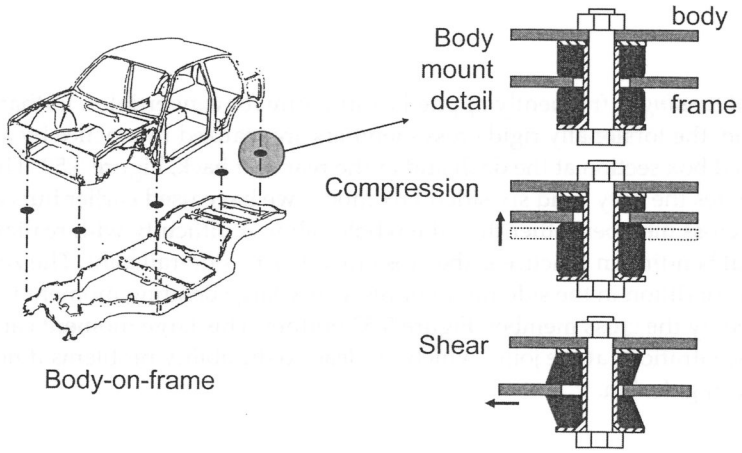

Figure 5.54 Body mounts.

If we consider a torque being applied to the frame though the suspension, the frame and body will tend to twist about different longitudinal axes, Figure 5.55. This type of twisting action causes shearing deformation in the body mounts, which reduces the stiffness of this system; the torsional stiffness of the vehicle can be less than the sum of the torsional stiffnesses of the body and the frame.

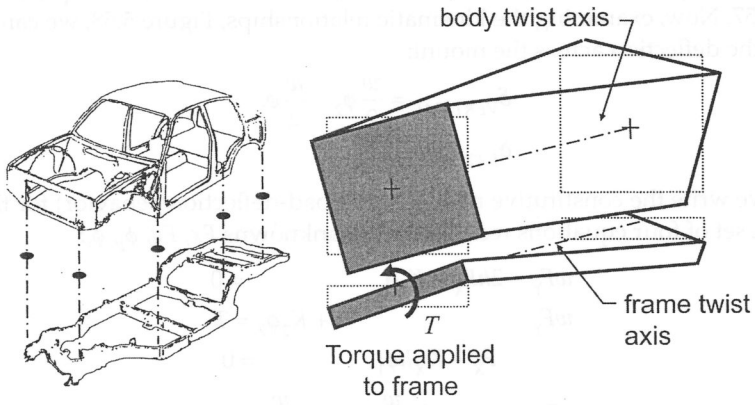

Figure 5.55 Body-on-frame idealized torsion model.

To understand how the frame, body, and body mounts combine to give a vehicle torsional stiffness, consider Figure 5.56a. Here we have the system of the body, with torsional stiffness K_1, the frame, with torsional stiffness K_2, and four body mounts at each corner, spaced by width, w, and length, L. The mount is viewed as two linear springs: one in the horizontal direction (shear stiffness k_X), and one in the vertical direction (compressive stiffness k_Y), Figure 5.56b.

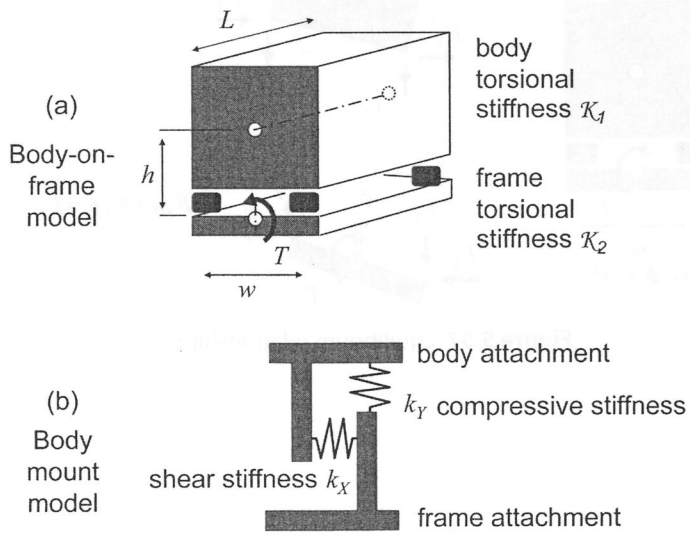

Figure 5.56 Torsion model definitions.

A torque, T, is applied at the front of the frame, Figure 5.57, with an equal and opposite torque applied at the rear. The frame then twists through ϕ_2 about its own twist axis in the plane of the frame, and the body twists through an angle ϕ_1 about its twist axis at height, h, above the frame. Note that ϕ_1 and ϕ_2 are very small angles so $sin\phi=0$ and $cos\phi=1$. The vehicle system can be exploded to show the internal loads, F_X and F_Y, and we can put both the body and frame into static equilibrium, Figure 5.57. Now, examining the kinematic relationships, Figure 5.58, we can identify the deflection across the mount:

$$\delta_{VERTICAL} = \frac{w}{2}\phi_2 - \frac{w}{2}\phi_1$$

$$\delta_{LATERAL} = h\phi_2$$

Finally, we write the constitutive relationship (load-deflection behavior) for the mount. A set of four equations result with the unknowns Fx, Fy, ϕ_1, ϕ_1:

$$\begin{aligned} wF_Y - 2hF_X - K_1\phi_1 &= 0 \\ wF_Y + K_2\phi_2 &= T \\ F_X - K_X h\phi_1 &= 0 \\ F_Y + K_Y\frac{w}{2}\phi_1 - K_Y\frac{w}{2}\phi_2 &= 0 \end{aligned}$$

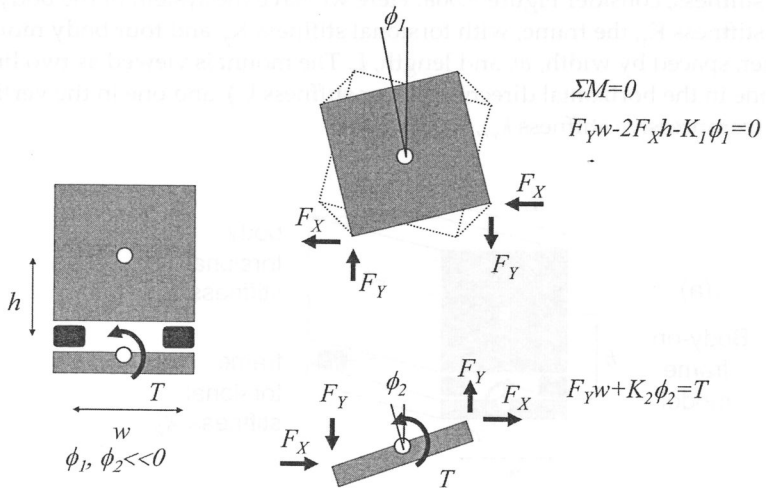

Figure 5.57 Equilibrium relationships.

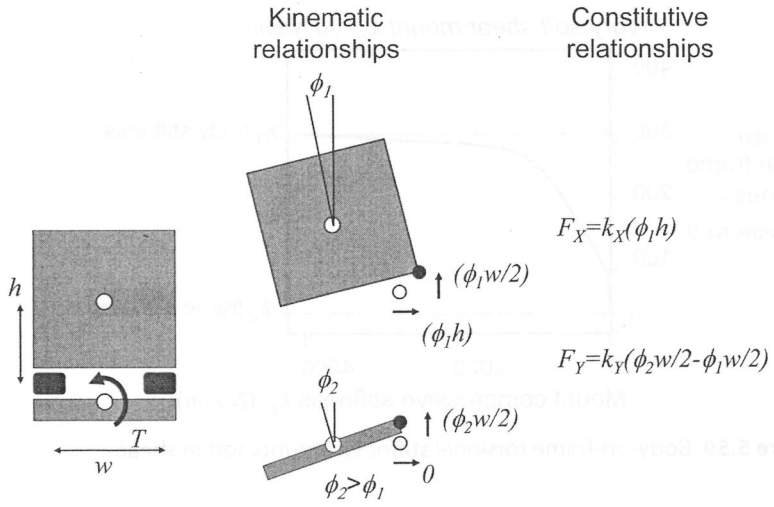

Figure 5.58 Kinematic and constitutive relationships.

We may solve this set and then take the ratio of T/ϕ_2 to arrive at the vehicle torsional stiffness, $K_{VEH}=T/\phi_2$:

$$K_{VEH} = K_2 + K_1\psi + 2h^2 k_X \psi$$

$$\psi = \frac{1}{1 + \dfrac{2h^2 k_X}{\left(\dfrac{w^2}{2} k_Y\right)} + \dfrac{K_1}{\left(\dfrac{w^2}{2} k_Y\right)}} \tag{5.18}$$

where:

K_1 and K_2 = Torsional stiffness of the body and frame, respectively,

k_X and k_Y = Mount stiffnesses in the horizontal and vertical directions

h = Height of the body twist axis above the plane of the frame,

w = Width between body mounts

ψ = Body-frame coupling term which indicates how tightly coupled are the twisting actions of the frame and body; larger ψ is greater coupling.

Equation 5.18 shows that the vehicle torsional stiffness consists of all of the frame stiffness, K_2, plus a portion of the body stiffness, $K_1\psi$, plus the unexpected term, $2h^2K_X\psi$. This last term depends on the shear stiffness, k_X, of the mounts. To understand this behavior, we take typical values for a body-on-frame sedan, and for the body mount select an extremely soft shear stiffness and vary the mount's compressive stiffness, Figure 5.59. Note that the frame torsional stiffness is typically very low in comparison to the body.

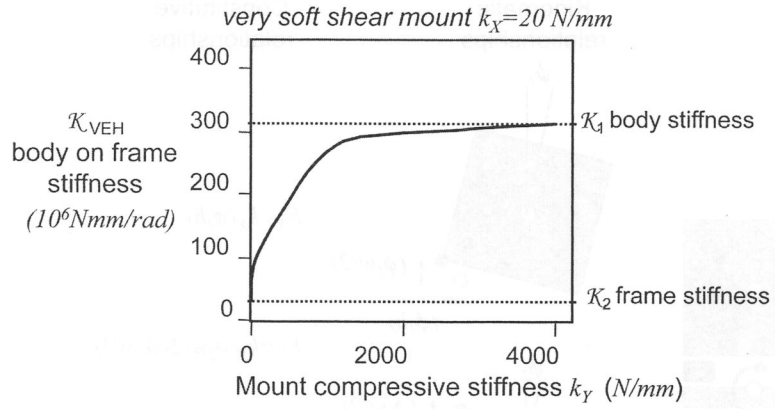

Figure 5.59 Body-on-frame torsional stiffness: Mounts soft in shear.

The resulting behavior, Figure 5.59, shows that for compressively soft mounts, the body is not coupled to the twisting motion of the frame and the vehicle stiffness approaches that of the frame alone. For compressively stiff mounts, the body and frame are highly coupled, and the vehicle stiffness approaches the sum of the body and frame stiffnesses.

Now using the same vehicle data, let us additionally vary the shear stiffness of the body mount. The result, Figure 5.60, shows that by increasing the shear stiffness of the body mounts, we can increase vehicle stiffness *beyond* the sum of the body and frame torsional stiffness. Physically, the reason for this is that the body and frame have different twist axes. By increasing the mount shear stiffness, the body and frame fight against one another for the axis to twist about. The combined twist axis is above the frame. As the combined twist axis moves above the frame, the frame itself becomes a shear-resistant member, Figure 5.61. This shearing of the frame contributes to a greater torsional stiffness for the vehicle system. Thus, the shear stiffness of the frame becomes an important design consideration.

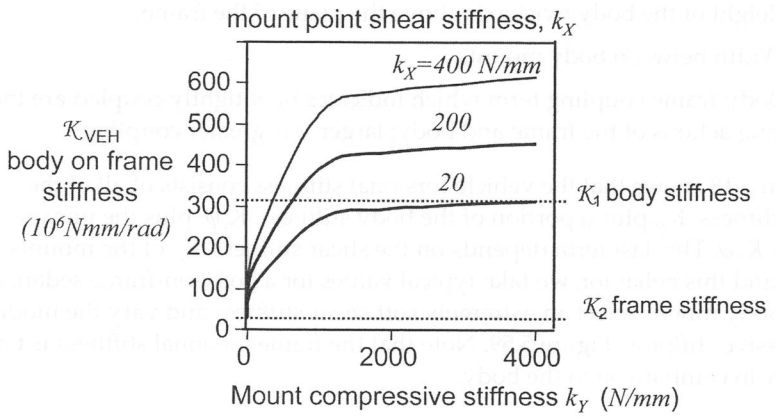

Figure 5.60 Body-on-frame torsional stiffness: Varying mount point shear stiffness.

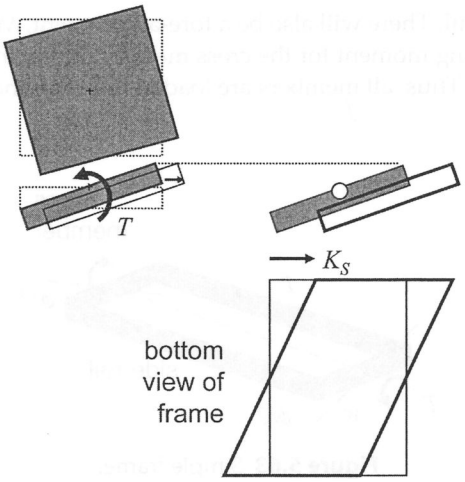

Figure 5.61 Shear of frame during torsion.

5.5.3 Torsional stiffness of a ladder frame

As discussed above, the ladder frame influences vehicle torsional rigidity not only by its *torsional stiffness* but also by its *shear stiffness*. In this section, we will look briefly at both of these conditions.

The evolution of the automobile frame, Figure 5.62, has tended towards closed sections for both side rails and cross members to improve torsional stiffness. Also, improved joints at the crossmember-to-siderail have improved both torsional and shear stiffness. To understand this evolution, let us look at a simple frame of two side rails and two cross members loaded at both ends by equal and opposite torques, Figure 5.63. Loaded in this way, at any section along the perimeter, there will be a moment in the cross vehicle direction, M_{zz}, as shown in Figure 5.64a. This moment acts as a uniform torque for the cross member, and a linearly varying bending

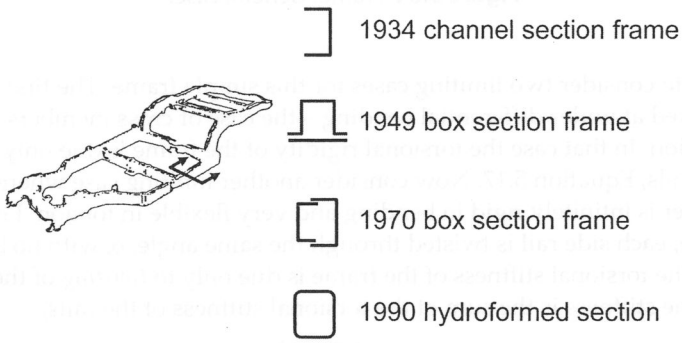

Figure 5.62 Typical frame configurations.

moment for the side rail. There will also be a fore-aft moment, M_{XX}, which will be a linearly varying bending moment for the cross member and a uniform torque for the side rail, Figure 5.64b. Thus, all members are loaded both in bending and in torsion.

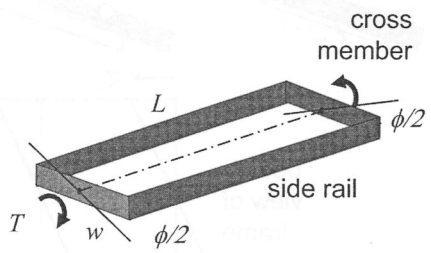

Figure 5.63 Simple frame.

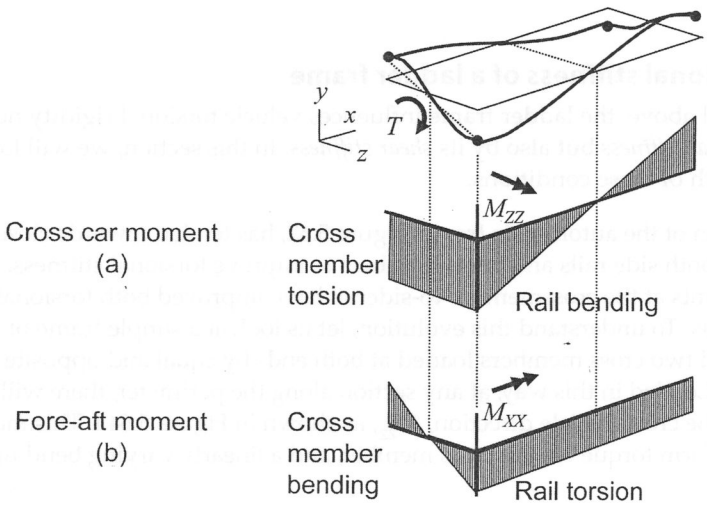

Figure 5.64 Frame: General case.

It is helpful to consider two limiting cases for this simple frame. The first we have already looked at under differential bending—the case of cross members being very rigid in torsion. In that case the torsional rigidity of the frame is due only to *bending* of the side rails, Equation 5.17. Now consider another limiting case where the cross member is infinitely rigid in bending and very flexible in torsion, Figure 5.65. For this case, each side rail is twisted through the same angle, ϕ, with no bending occurring. The torsional stiffness of the frame is due only to *twisting* of the side rails, and the frame stiffness is the sum of the torsional stiffness of the rails,

$$K = 2\left(\frac{GJ_{EFF}}{L}\right) \tag{5.19}$$

where:

G = Shear modulus

J_{EFF} = Torsion constant of side rail

L = Length of side rail

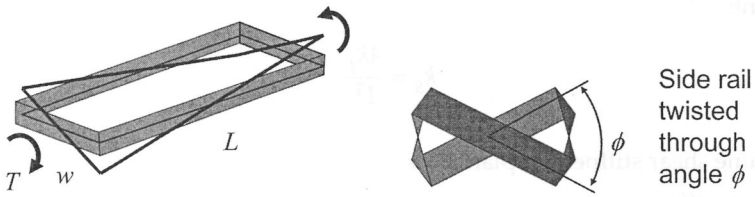

Figure 5.65 Cross members infinitely rigid in bending and very flexible in torsion.

In these two limiting cases, we see that both twisting as well as bending of the side rails can add to the frame torsional stiffness. (We could have considered these limiting cases with the side rails as infinitely stiff, and drawn parallel conclusions about bending and twisting of the cross members.)

For the general case of frame torsion, both the cross members and side rails are under both bending and torsion, as in Figure 5.64. A Finite Element Analysis may be used to understand the relative contribution of each of these conditions. Figure 5.66 shows data for a generic planar frame of steel with section size *100 mm (4 in.)* square and *1 mm (0.04 in.)* thick. A torsional stiffness of *2030 Nm/° (1500 ft lb/°)* results with the strain energy distribution shown. The torsion strain energy is larger than the bending strain energy for both the cross members and the side rails. This implies that increasing the torsional properties would have the largest influence on frame stiffness. This sensitivity to torsional section properties is typical for most common automotive frames. Note also the relatively low torsional stiffness value compared with the typical monocoque body values of *10,000–12000 Nm/o (7375–8850 ft lb/°)*.

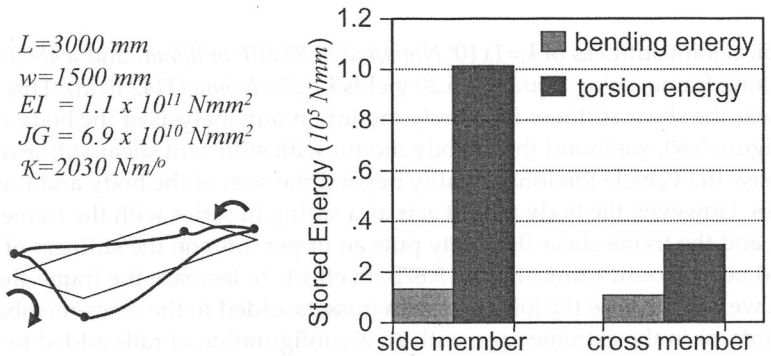

Figure 5.66 Strain energy in frame under torsion.

Finally, in discussing body-on-frame torsional behavior, the importance of frame shear stiffness, k_S, was pointed out, Figure 5.61. This plan-view shearing stiffness depends greatly on the crossmember-to-siderail joints, Figure 5.67a. As an approximation for describing this stiffness, consider a frame consisting of rigid beam elements connected by flexible joints with stiffness, k_J. Loading the frame in shear with a load, F, a deflection, δ, will result. Using energy principles, we can write the shear stiffness of the frame, k_S, as seen at each body mount attachment:

$$k_S = \frac{4k_J}{L^2} \tag{5.20}$$

where:

k_S= Frame shear stiffness in plan view

k_J = Joint stiffness

L = Length of side rail

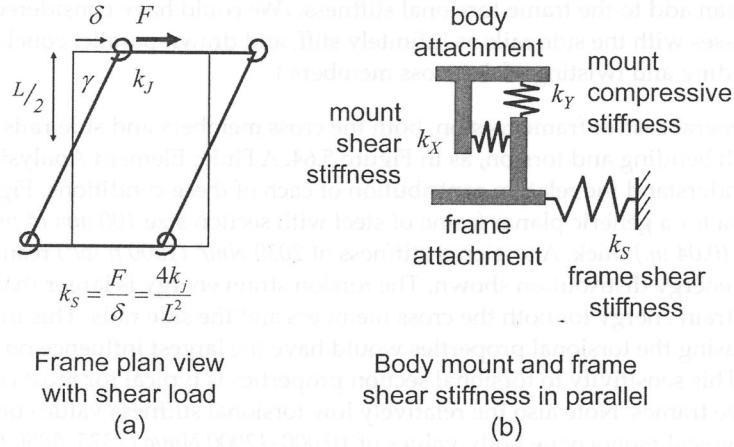

Figure 5.67 Frame shear stiffness as seen at mount attachment.

For a typical joint stiffness of k_J=*1x10⁹ Nmm/rad (8.85x10⁶ in lb/rad)* and a *4500 mm (177 in.)* long frame, using Equation 5.20 yields k_S≈*200 N/mm (1142 lb/in)*. This value is very near the shear stiffness for a body mount. In our analysis of the body-on-frame, Figure 5.60, we found that a body mount with sufficient shear stiffness can increase the vehicle torsional rigidity beyond the sum of the body and frame stiffnesses. However, the body mount acts as a spring in series with the frame shear stiffness, and the frame shear flexibility puts an upper limit on the stiffness of the combined body mount-frame, Figure 5.67b. In efforts to increase the frame shearing stiffness, we can increase the joint rate with gussets added to the cross-member-to-rail joints, or in the extreme case, with an *X* configuration of rails added to the frame, Figure 5.68.

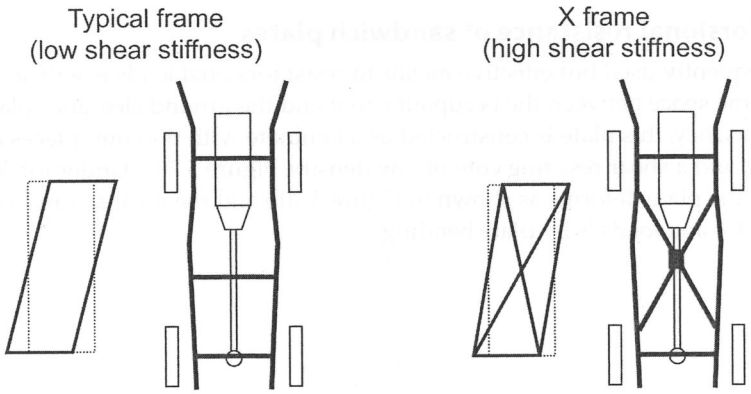

Figure 5.68 Shear stiffness of frame.

5.5.4 Torsional stiffness of backbone frame vehicles

For cases where vehicle packaging allows, a large central closed section can be a very effective structure for torsional stiffness. Usually this structure arrangement is limited to seating arrangements where a large high tunnel can be tolerated, such as open two-seat sport cars. For preliminary sizing of a backbone structure, the equations for closed thin-walled sections may be used for both strength and stiffness estimates, Figure 5.69. As these sections tend to have large width-to-thickness ratios, careful attention must be paid to elastic shear buckling of the walls. Frequently, diagonal rib patterns on the backbone sides are used to inhibit shear buckling.

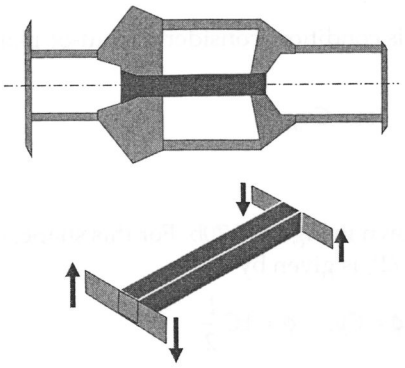

$$\theta = \frac{TL}{GJ_{EFF}}$$

$$J_{EFF} = \frac{4A_{ENCLOSED}^2 t}{S}$$

$$\tau = \frac{T}{2A_{ENCLOSED}t}$$

Figure 5.69 Backbone frame.

5.5.5 Torsional resistance of sandwich plates

An infrequently used but effective means to resist torsional loads is with a thick plate in the space between the occupant's foot and the ground clearance plane. For mass efficiency, this plate is constructed as a laminate with thin outer faces of a stiff material, and a shear resisting core of low density, Figure 5.70a. Under torsional loading, the plate deforms as shown in Figure 5.70b and the means of reacting the external torsion loads is by plate bending.

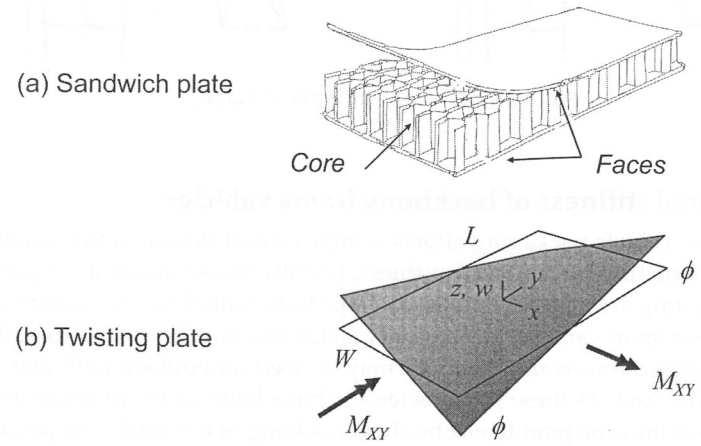

Figure 5.70 Under-floor thick plate.

To develop a first-order model of this condition, consider the out-of-plane deflection at a point, *(x,y)*, to be given by

$$w = Cxy$$

where C = a constant

This describes the twisted shape shown in Figure 5.70b. For this shape, the angle of rotation at each end of the plate, *(±L/2)*, is given by

$$\frac{\partial w}{\partial x} = \phi = Cy, \quad \phi = \pm C\frac{L}{2}$$

or the total angle of rotation, θ, for the plate from front to rear is

$$\theta = 2\phi = CL$$

Now consider the applied moments required to distort the plate into this shape. Using the plate equations from Equation 3.21, the moments depend on the second partial derivatives of the deflection function above:

$$\frac{\partial^2 w}{\partial x^2} = 0, \quad \frac{\partial^2 w}{\partial y^2} = 0, \quad \frac{\partial^2 w}{\partial x \partial y} = C$$

$$M_X = -D\left(\frac{\partial^2 w}{\partial x^2} + \mu \frac{\partial^2 w}{\partial y^2}\right) = 0$$

$$M_Y = -D\left(\mu \frac{\partial^2 w}{\partial x^2} + \frac{\partial^2 w}{\partial y^2}\right) = 0$$

$$M_{XY} = -D(1-\mu)\left(\frac{\partial^2 w}{\partial x \partial y}\right) = -DC(1-\mu)$$

So, not surprisingly, the applied moment along all edges is the twisting moment, M_{XY}, per unit of edge length, Figure 5.70b. A means to interpret this moment is to divide the plate along each side into small, equal increments of width and length, Δx and Δy, Figure 5.71a. Now consider a series of couples applied along each edge of the plate of magnitude $F\Delta x$ along the width and $F\Delta y$ along the length. These couples provide the twisting moment, M_{XY}, according to:

$M_{XY}\Delta x = F\Delta x$ along the width, and $M_{XY}\Delta y = F\Delta y$ along the length.

The magnitude of these forces is therefore

$$F = M_{XY}$$

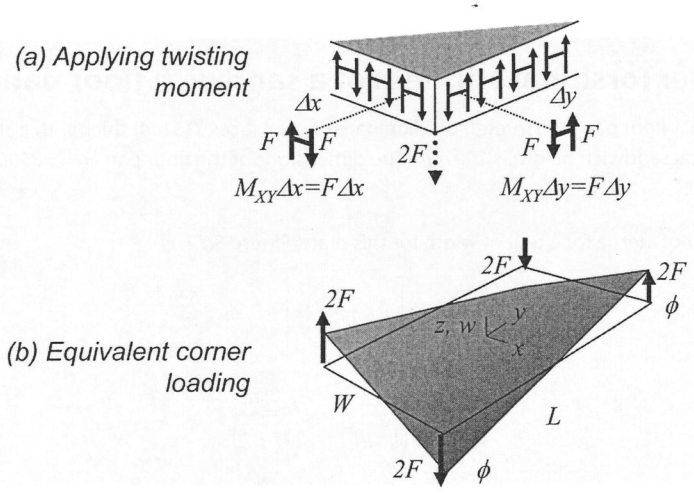

Figure 5.71 Plate twisting.

Now consider this series of up and down forces along the edges of the plate, Figure 71a. The forces cancel in up-down pairs except at the corners of the plate where they sum to a corner force of $2F$. Thus an equivalent loading for the plate is by corner forces, Figure 5.71b, with magnitude

$$2F = 2M_{XY} = 2DC(1-\mu)$$

So the twisting couple acting on the plate is

$$T = (2F)W = 2DC(1-\mu)W$$

The torsional stiffness for a general plate is then

$$K = \frac{T}{\theta} = \frac{2DC(1-\mu)W}{CL} = 2D(1-\mu)\frac{W}{L} \tag{5.21}$$

where:

K = Torsion stiffness of a plate

$$D = \frac{EI}{(1-\mu^2)}$$

W = Plate width

L = Plate length

In the example below, we will consider the specific case of a sandwich plate with very stiff material (high E) for the faces, and a much more flexible material (low E) but shear resistant for the core.

Example: Torsional stiffness of a sandwich floor pan

Consider a flat floor pan constructed of a laminate of steel faces, *0.5 mm* thick with a shear-resistant core. The total sandwich height is *100 mm*. The dimensions of the floor pan are *L=3500 mm, W=1500 mm*.

The moment of inertia for a unit of width for this plate, Figure 5.72, is

$$EI = E_{FACE}\left[2(t\cdot 1)\left(\frac{h}{2}\right)^2\right] = \frac{E_{FACE}th^2}{2}$$

$$D = \frac{EI}{(1-\mu^2)} = \frac{E_{FACE}th^2}{2(1-\mu^2)}$$

$$K = \frac{2D(1-\mu)W}{L} = 2\left[\frac{E_{FACE}th^2}{2(1-\mu)(1+\mu)}\right](1-\mu)\frac{W}{L}$$

$$K = \frac{E_{FACE}th^2}{(1+\mu)}\frac{W}{L} \tag{5.22}$$

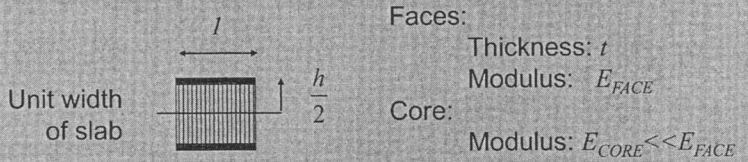

Figure 5.72 Moment of inertia for sandwich.

Where Equation 5.22 is the stiffness of a sandwich laminate. Substituting values for this example,

$$K = \frac{(207000N/mm^2)(0.5mm)(100mm)^2}{(1+.3)}\frac{1500mm}{3500mm}$$

$$K = 341{,}200{,}000Nmm/rad(5986Nm/o)$$

This value is a large fraction of our nominal vehicle torsional stiffness of *12000 Nm/°*, and shows the effectiveness of this structural system. Of course, a load path from the suspension attachments to this plate must be provided to realize this stiffness.

References

1. Milliken, W. & Milliken, D., *Chassis Design, Principles and Analysis*, SAE International, Warrendale, PA, 2002, pp. 93–101.
2. Gillespie, T. D., *Fundamentals of Vehicle Dynamics*, SAE International, Warrendale, PA, 1992, pp. 210–214.
3. Fenton, J., *Vehicle Body Layout and Analysis*, Mechanical Engineering Publications, Ltd, London, 1980, p. 93.
4. Pawlowski, J., *Vehicle Body Engineering*, Business Books, London, 1969, pp. 149–150.
5. Brown, J.C., Robertson, A. J., Serpento, S.T., *Motor Vehicle Structures*, SAE International, Warrendale, PA, 2001, pp. 75–84.
6. Kikuchi, N. & Malen, D., Course notes for ME513 Fundamentals of Body Engineering, University of Michigan, Ann Arbor, MI, 2007.